J Sol-Gel Sci Technol (2017) 81:378–404
DOI 10.1007/s10971-016-4197-7

REVIEW PAPER: FUNCTIONAL COATINGS, THIN FILMS AND MEMBRANES (INCLUDING DEPOSITION TECHNIQUES)

Dip-coating for fibrous materials: mechanism, methods and applications

Xiaoning Tang[1] · **Xiong Yan**[1]

Received: 5 July 2016 / Accepted: 26 August 2016 / Published online: 20 September 2016

Abstract This paper presents a review on dip-coating for fibrous materials, mainly concentrated on the mechanism, recently developed dip-coating methods and novel functional applications. The emphasis has been made here, to present theoretical basis of dip-coating-induced film deposition, especially, the reported works to predict the thickness based on various processing parameters. Different modified dip-coating techniques to fabricate deposited films for fibrous substrate have also been gathered. The scope of reviewed dip-coating methods are not only conventional solution and sol–gel-based dip-coating, but also recently developed vacuum-assisted, spin-assisted, photo-assisted and multi-layered dip-coating methods. An overview of reported and potential applications for coated fibrous materials has also been given, which mainly including self-cleaning, oil–water separation, conductive textiles, fibrous-based energy storage devices, and photonic crystals, etc. This review is intended to give readers a good horizon for the present status concerning variety of studies and applications related to dip-coating. An effort has been made here to report the important contributions in the area of dip-coating for fibrous substrate, and critical points regarding future research directions are outlined in the summary.

Graphical Abstract

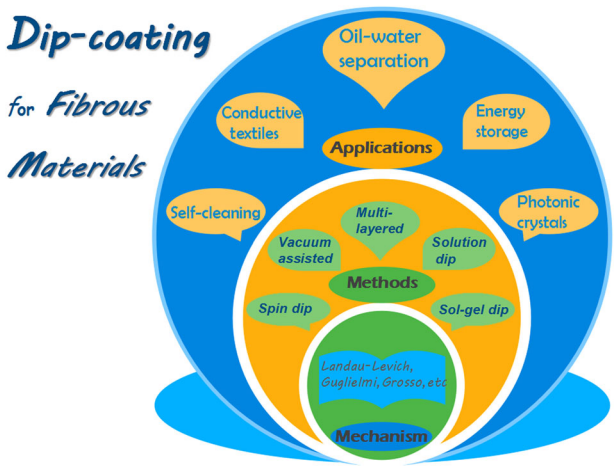

Keywords Dip-coating · Fibrous materials · Sol–gel · Self-cleaning · Energy storage

1 Introduction

Dip-coating is a facile and economical technique widely used in many industrial fields to deposit onto any substrate, including metallic, ceramic, polymer films ,and fibrous materials, etc. The process could be defined as depositing aqueous-based liquid phase coating solutions onto the surface of any substrate. Generally, target materials are dissolved in solutions which directly coated on the surface of substrate, then the sedimentary wet coating has been evaporated to obtain dry film [1–3]. The approach involves immersing a substrate into the solution of coating

✉ Xiaoning Tang
tangxn123@163.com

✉ Xiong Yan
profyaxi@yeah.net

[1] Key Laboratory of Textile Science and Technology, Ministry of Education, College of Textiles, Donghua University, Shanghai 201620, China

materials, therefore ensure that the substrate has been fully infiltrated and then withdraw from the solution tank. It should be noted that this seemingly simple formation process of film via dip-coating involves complex chemical and physical multi-variable parameters. During dipping and coating, the thickness and morphology of depositing thin films were determined by many parameters such as immersion time, withdrawal speed, dip-coating cycles, density and viscosity, surface tension, substrate surface and evaporation conditions of coating solutions, etc.

Considering the good machinability and widespread applications of dip-coating, it has been an increasing topic in both fluid physics and interface science. The earliest studies of dip-coating were implemented by directly solution dipping and coating process, thus improve the surface properties of fibrous materials. Sol–gel-based dip-coating is a primary modification of solution dip-coating, and the deposited films could be better controlled by regulating the preparation of sol and subsequent gelation process [4, 5]. Furthermore, developed spin-assisted and vacuum-assisted dip-coating techniques are efficient to improve the infiltrating between coating solutions and fibrous substrate. Photo-assisted dip-coating was also applied to control the coating solution evaporation process, due to the irradiation effect is beneficial to facilitate film disposition. Multi-layered dip-coating was firstly studied to increase the uniformity and thickness of deposited films, recently it shed light in the functionalization of fibrous materials. Different coating solutions were alternately deposited onto the surface of fibrous substrate, thus achieving the desired functionality. The initial purpose of dip-coating to improve the mechanical properties, abrasive resistance, spinnability, and weavability of fibrous-based materials, which were not the scope of this review. The present work was more concentrated on the potential functionality of coated fibrous materials, including the reported self-cleaning, separation, e-textiles, fibrous-based energy devices, and photonic crystals, etc.

Herein, it is a description of dip-coating for fibrous materials, including the mechanism, modified dip-coating techniques and various functional applications of coated fibrous materials. The purpose of this review is to introduce the characteristics and theoretical basis of dip-coating, and show the state of the art for various dip-coating techniques. Furthermore, the applications of coated fibrous materials in the fields, such as self-cleaning textiles, oil-water separation, electrical conductive e-textiles, and fibrous-based energy storage devices were gathered. It is hoped that this review will give motivation for both the development of novel dip-coating manufacturing methods and promising application prospects of coated fibrous materials.

2 Mechanism and theoretical basis of dip-coating

One of the most important aspect of dip-coating process is the thickness of deposited films, which is the basis of various physical, chemical properties and applications. It is known that various parameters, including dip-coating time, withdrawal speed, coating solution concentration, composition and temperature have strong influence on the thickness of deposited films. A series of papers have been published to investigate the effect of processing parameters on the thickness of deposited coatings [6–10]. Whatever the coating approach, efforts were made to understand the dip-coating mechanism, which both fibrous surface and coating solutions coexist in the film deposition process. Initially, various empirical equations have been developed to exploit the characteristics of coatings, but the results usually proven to be paradoxical due to the complex factors.

Furthermore, several theoretical formulas were established to solve this problem, such as the famous Landau-Levich theory, which predict the thickness of deposited films via the following equation:

$$t_1 = 0.944 C_a^{1/6} \left(\frac{\eta U}{\rho g}\right)^{1/2} \tag{1}$$

where C_a is the capillary number and given by $C_a = \eta U/\delta$; η, δ, and ρ denote viscosity, surface tension, and the density of coating solutions, respectively; U is the withdrawal speed and g is the gravitational acceleration constant. Groenveld also constructed a model to estimate the thickness which emphatically considered the flow, the resulting equation as follows:

$$t_1 = J \left(\frac{\eta U}{\rho g}\right)^{1/2} \tag{2}$$

where J is the dimensionless flow. It should be noted that both eqs.1 and 2 are valid in the case of $C_a < 10^{-3}$ and for *Newtonian* fluid. To investigate the dip-coating process of high viscosity solutions such as sol-gel dipping, Guglielmi and Zenezini [11, 12] established the following equations:

$$t_1 = t_p \frac{\rho_p}{c} \tag{3}$$

$$t_p = 0.944 C_a^{1/6} \frac{c}{\rho_p} \left(\frac{\eta U}{\rho g}\right)^{1/2} \tag{4}$$

$$t_p = J \frac{c}{\rho_p} \left(\frac{\eta U}{\rho g}\right)^{1/2} \tag{5}$$

where t_p is heat-treated coating thickness, ρ_p is the density of heat-treated coating (g cm^{-3}) and c is the concentration of coating solutions (g cm^{-3}). Dimensionless flow J should be experimentally determined and measured, and various thickness of coatings could be obtained by changing the

concentration of solutions and withdrawal speeds. Young and coworkers [13] reported that the increasing concentration of erbium acetate coating solutions results in an increase of coating layer thickness, and the thickness of coating layer is positively related to the viscosity of coating solutions. In addition, the increasing erbium oxide rate also increases the coating solutions, lower velocity of coating solutions fluid drainage results in the thicker coating layer. The reason could be explained that the higher viscosity, the slower coating liquid moves downward. The obtained model provides reasonable trends for coating thickness on planar substrate under the gravity-driven drainage and evaporation of coating solvent.

The parameters such as withdrawal speed, dip-coating time, coating temperature, and distance are gradually interesting to investigate the mechanism and processing conditions. For instance, Roland and coworkers [14] observed that the average thickness decrease with dip-coating rate in certain range, which is suitable to films dip-coated from solutions of all NCOOH/VP molar ratios as shown in Fig. 1a. Figure 1b described the curves for $CHCl_3$, THF, toluene, and dioxane solvent, which contain 10 mg mL^{-1} PS-P4VP with equimolar NCOOH. The results confirmed that the deposited films varies with dip-coating rate as a V-shaped wave [14]. The works of Faustini et al. [16] further confirmed this tendency, and the slope of curves varied with different processing parameters, including the coating solution properties, substrate and evaporation conditions, as shown in Fig. 1c. For thickness could be described by the sum of the contribution of each regime, which leads to semi-experimental model shown in Fig. 1d inset. It links the final thickness to the coating solution properties and processing conditions, which is mainly composed of solution composition constant (K_i), rate of evaporation *(E)* divided by the product of speed u times the dimension L of the substrate (represented as $E(Lu)^{-1}$) and

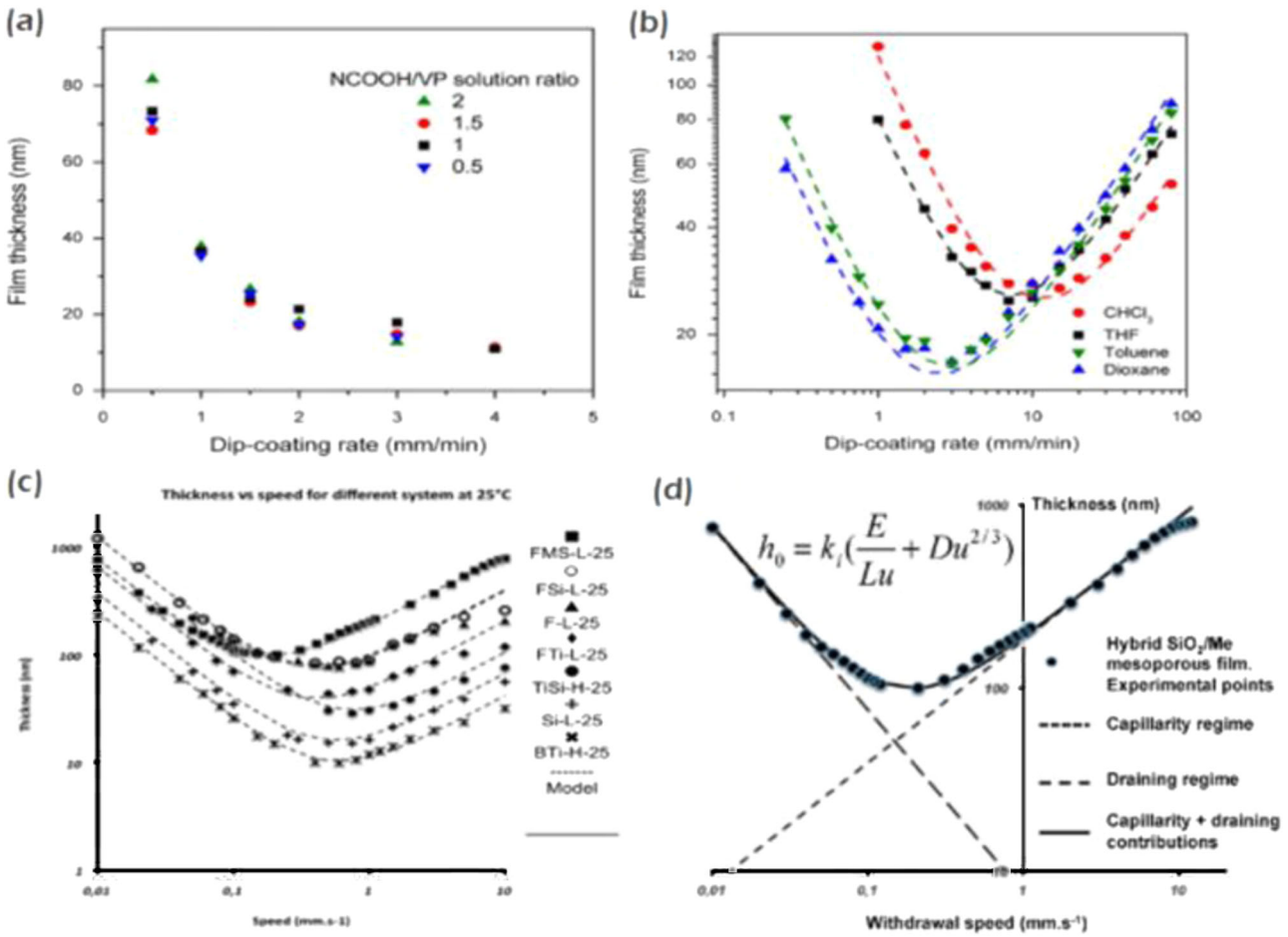

Fig. 1 **a** Thickness of films dip-coated from the NCOOH/VP solutions with different molar ratios [14]; **b** film thickness as a function of dip-coating rate (withdrawal speed) from CHCl3, THF, toluene and dioxane solvent, respectively [15]; **c** evolution of thickness versus withdrawal speed for various coating systems formed at room temperature [16]; **d** typical thickness vs. dip-coating speed curve of a sol–gel film [17]. **a** Copyright 2012, American Chemical Society; **b** copyright 2015, American Chemical Society; **c** copyright 2006, American Institute of Physics; **d** copyright 2014, American Chemical Society

solution physical chemical characteristic *(D)* times the speed $u(Du^{2/3})$, which describes the viscous drag regime of deposition [17]. Furthermore, it has been indicated that the typical log-log evolution of thickness vs. withdrawal speed, and main regimes of deposition are clearly visible under extreme conditions, while minimum thickness could be obtained for intermediate regime.

The approximately V-shaped dependence of film thickness on dip-coating rate could be explained by the combination of two reported competitive dip-coating regimes [16, 18]. A semi-experimental equation has been reported by Grosso and coworkers to investigate the effects of chemical and dynamic processing conditions on the fabricated membrane deposited on the surface of fibrous materials [15–17]. The established model emphatically considered the intrinsic characteristics of coating solutions covering both the capillarity and draining regimes, which is an additional important parameter affecting the film thickness. The capillarity regime theory indicated that the minimum of slow dip-coating, which is governed by capillarity feeding of the developing film as solvent evaporates, thus leading to thicker films as dip-coating rate decreases. And the draining regime dominating the high dip-coating side of the minimum, that is the usual regime used for dip-coating, where film thickness increases with dip-coating rate. The equation has been verified for metallic, ceramic, polymeric, and porous substrates, and the regime schematic diagram could be seen in Figs. 2a–c [16]. However, for sol-gel-based dip-coating, the films deposition process normally starts with a coating solutions composed of ethanol, water, silica, and various surfactants mixture. The withdrawal speed should be sufficiently low to ensure the proper balance between substrate surface and multiple component coating solutions. The factors concerning the deposition of films, including the evaporation of solvent, self-assembly of micelles and inorganic phase, and the condensation of deposited networks, as shown in Fig. 2d [19].

For the dip-coating process with extremely low withdrawal rate, coating solvent was evaporated from the edge of meniscus and then the coating solution is raised to the edge of the meniscus by capillary force. The phenomenon of coating solutions induced by capillary flow is commonly known as the coffee-ring effect, and the edge of the coating solution is pinned to the substrate due to upward capillary flow. Higher coating temperatures could effectively facilitate the capillary flow of coating solutions, thus resulting in larger thickness of deposited films, as shown in Fig. 3a for silica-PVP hybrid films [20]. The evolution of of coating solutions evaporation rate vs. temperature is shown in Fig. 3b–d, which displays minimum thickness (h_{min}), experimental value of solution consuming rate (E/L) and critical speed (u_c) vs. temperature in three studied systems, respectively [16]. It should be noted that temperature has a similar slope for three systems, and evaporation dominates the formation of film due to capillarity feeding.

The cross linking conditions of coating solutions and coating times have also been investigated, the results of deposited layer thickness as a function of dipping time could be seen from Fig. 4. For covalently cross-linked mussel-inspired dendritic polyglycerol coatings as shown in Fig. 4a [21], the films quickly increased and reached approximately 60 nm after 10 min and a maximum thickness of 3.4 μm after 4 h on silica substrates. However, the thickness of coordination-based coating solutions just reached 10 nm after 12 h of deposition, as observed from Fig. 4b, which was due to the fewer cross-linking groups and relatively weak bonding conditions [21].

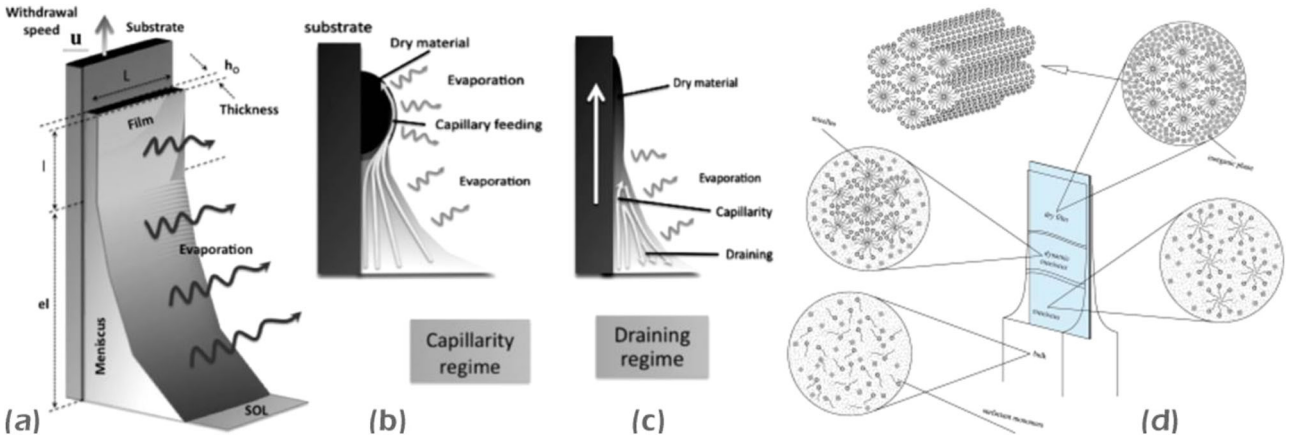

Fig. 2 **a**–**c**. Schemes of the dip-coating method for both capillarity and draining regimes at low and fast withdrawal speeds, respectively [16]; **d** the dip-coating set up illustrates the surfactant templating mechanism. Both micelle alignment and self-assembly of micelles with the inorganic phase occur in and above the dynamic meniscus region within a short time scale [19]. **a**–**c** Copyright 2010, American Chemical Society; **d** copyright 2006, American Institute of Physics

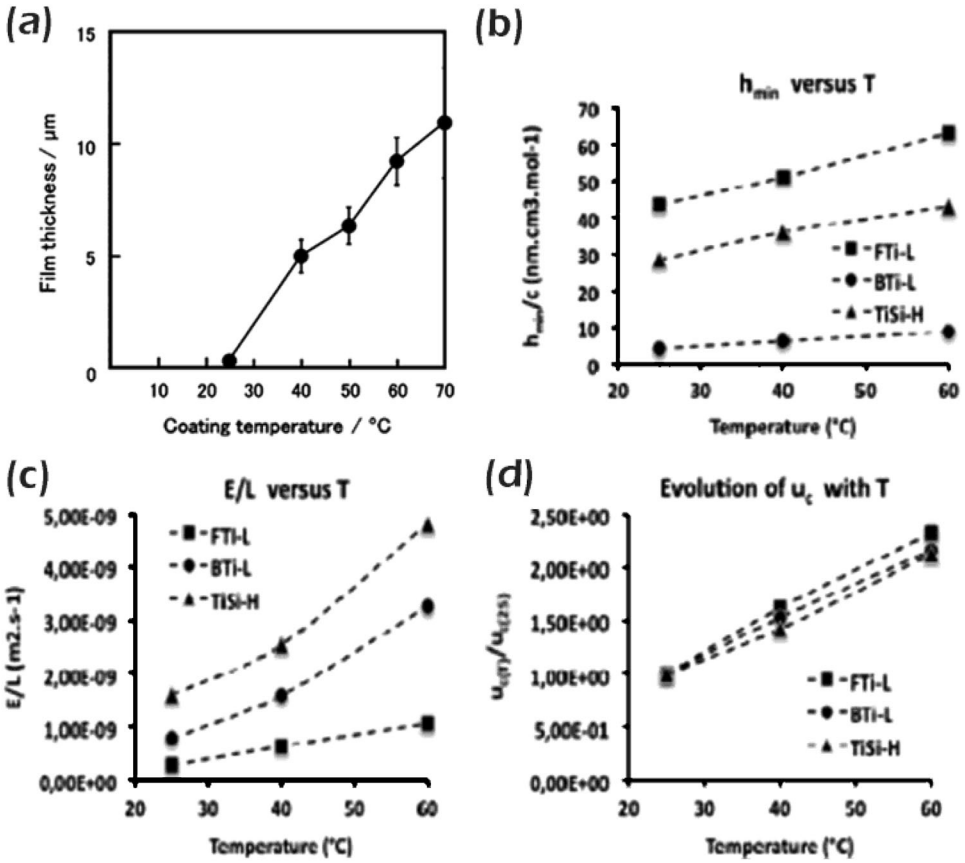

Fig. 3 **a** Dependence of film thickness on coating temperature for the silica-PVP hybrid films [20]; Evolution of (**b**) the minimal thickness (h_{min}), **c** the solution consuming rate (E/L), and **d** the relative critical withdrawal speed with temperature for different systems. *Dashed* lines are added as guides to the eye [16]. **a** Copyright 2012, Royal Society of Chemistry; **b**–**d** copyright 2010, American Chemical Society

Fig. 5a shows the curves of thickness vs. distance for graded mesoporous titanium oxide films under varying dip-coating speed from 0.2 to 10 s^{-1} [22]. Further, the thickness under different distance conditions at 10 s^{-1} with different dilutions as shown in Fig. 5b, and the results could be explained by the combined effect of viscosity and evaporation for concentrated coating solutions. Fig. 5c displays the experimental and predicted thickness of graded films following linear, logarithmic, or square power increases along with the dipping distance from an initial withdrawal speed[22]. The approach was also generalized to other systems as shown in Fig. 5d, where linear graded films made from sol–gel-derived silica, colloidal metal-organic framework ZIF-8, and PS-b-PEO block copolymer, respectively [22]. In particular, the fabrication of these gradient films were performed via dip-coating under optimized conditions, and thickness-dependent self-assembly process was investigated.

Compared with the precision deposition methods mainly for highly uniform metallic layer, such as chemical vapor disposition, physical vapor disposition, atomic layer disposition, and sputtering disposition, dip-coating show unique advantages in fibrous materials coatings. Almost any aqueous coating solutions could be easily deposited on substrate surface if proper processing conditions are applied. The dip-coating process don't need special equipment, and films could be successfully fabricated even in the most simple laboratory conditions. Furthermore, it is particularly suitable for the continuous industrial production of large area membrane-coated fibrous materials, such as filament, yarn, and fabric, etc. Fibrous materials coated by dip-coating approach have been widely used in the application of hydrophobic, electric conductivity, antibacterial, separation, transducer, drug delivery systems, and energy devices. However, the porosity of fibrous materials is intrinsically an obstacle for the precise control of thickness and structure compared with metallic or ceramic substrates. Currently, not much effort has been dedicated to solve this problem even the interaction process between fibrous substrates and coating solutions has not been fully understand.

3 Methods of dip-coating for fibrous materials

In this section, various modified dip-coating techniques to fabricate deposited films onto fibrous substrate surface have also been provided. The scope of gathered dip-coating methods, including facile solution dipping, sol-gel-based dip-coating, vacuum-assisted, spin-assisted, photo-assisted, and multi-layered dip-coating methods. The basic

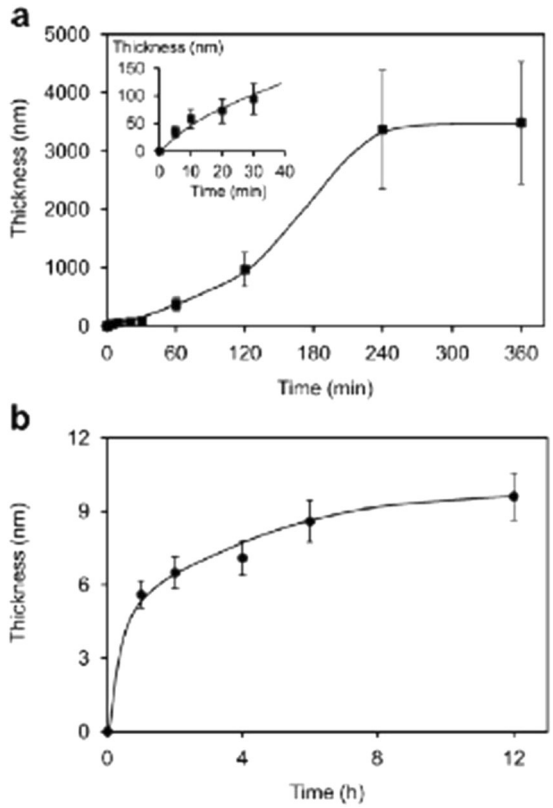

Fig. 4 Time-dependent thickness of the (**a**) covalently and (**b**) coordinatively cross-linked mussel-inspired dendritic polyglycerol coatings on silica surfaces [21]. Copyright 2014, Wiley

characteristics of various dip-coating methods as shown in Table 1.

3.1 Directly solution dip-coating

Solution dip-coating is the simplest technique for film disposition on fibrous materials surface and is generally used in scale-up coating production. As one of the most widely used process in textile manufacturing, dip-coating is also called starch finishing or sizing. During this approach, yarns or filaments are dipped into sizing agent solutions to increase the strength and reduce the breakage for subsequent weaving. This solution dip-coating process also shed light in tailoring the interfacial properties of fiber reinforced composites. It has been reported that self-assembled graphene oxide interlayers are easily fabricated by solution dip-coating infiltration for carbon fiber reinforced polyimide composites [33]. Carbon fabric reinforced phenolic composites modified with potassium titanate whisker (PTW) were also prepared by a solution dip-coating technique, and assisted with ultrasonic processing and heating to evaporate the solvent [23]. Furthermore, porous interfacial region could also be fabricated by dipping fibers into monoclinic ZrO_2 suspensions, where different particle size were taken to tailor porosity [34]. The modified interfacial region could also overcome interfacial incompatibility issues in fiber reinforced composites. It has been demonstrated that the interfacial properties of cellulose-based bio-composites could be tailored through deposition process from solution onto the cellulose substrate carried out by simple dip-coating. The schematic diagram of the fabrication procedure used in this work in presented in Fig. 6 [35]. The fabrics were dipped into the aqueous solutions of poly (ethylene glycol)-based amphiphiles, and then dried in vacuum drying chamber. Afterwards, the composites were produced by compression molding via a stacking procedure using square samples of pretreated fabrics [35]. Ni catalyst could be deposited on the fiber surface using electroless dip-coating method, which is beneficial to the growth of CNTs, thus improve the storage modulus and interfacial shear stress [36]. Therefore, it can be concluded that solution dip-coating is an efficient method for mechanical improvement and functional fabrication of composites materials through interfacial tailoring.

Recently, it has been reported that the resistance of electrical conductive cellulose-based fibers could be controlled in a wide range by varying the parameters of dip-coating into CNTs solutions [24]. Lotus effect could be also achieved by two-step dipping process into silica microsphere suspension and silica sol, respectively, which is time-saving and multi-shape applicable [37]. Similarly, zinc oxide films was successfully grown on cotton fibers surface via dipping into zinc chloride, and subsequent zinc acetate aqueous solution with alkaline drops continuously added under magnetic stirring [38]. Solution dip-coating is an efficient method to improve the bio-compatibility of fibrous materials, such as the reported hydroxyapatite/chitosan nanohybrid coatings on porous carbon fiber felts [39] and biologically active chitosan-coated lyocell fibers [40]. Apart from mostly studied aqueous solutions, poly(methyl methacrylate) was also taken as dipping solutions, for instance, the reported poly(methyl methacrylate)-based coatings incorporated with hydroxyapatite applied for ultra high molecular weight polyethylene [41, 42]. Compared with conventional aqueous solutions, poly(methyl methacrylate) showed the unique advantages such as excellent adhesivity and tribological performance. In addition, metal-organic precursor was coated on the end of single optical fiber by solution dip-coating process, and then decomposed in a propane flame to prepare high-resolution fiber-optic interferometer [43]. The method is fast and easy in comparison with commonly used physical sputtering deposition and thermal evaporation methods, and is a promising technique in the fabrication of high performance fibrous materials.

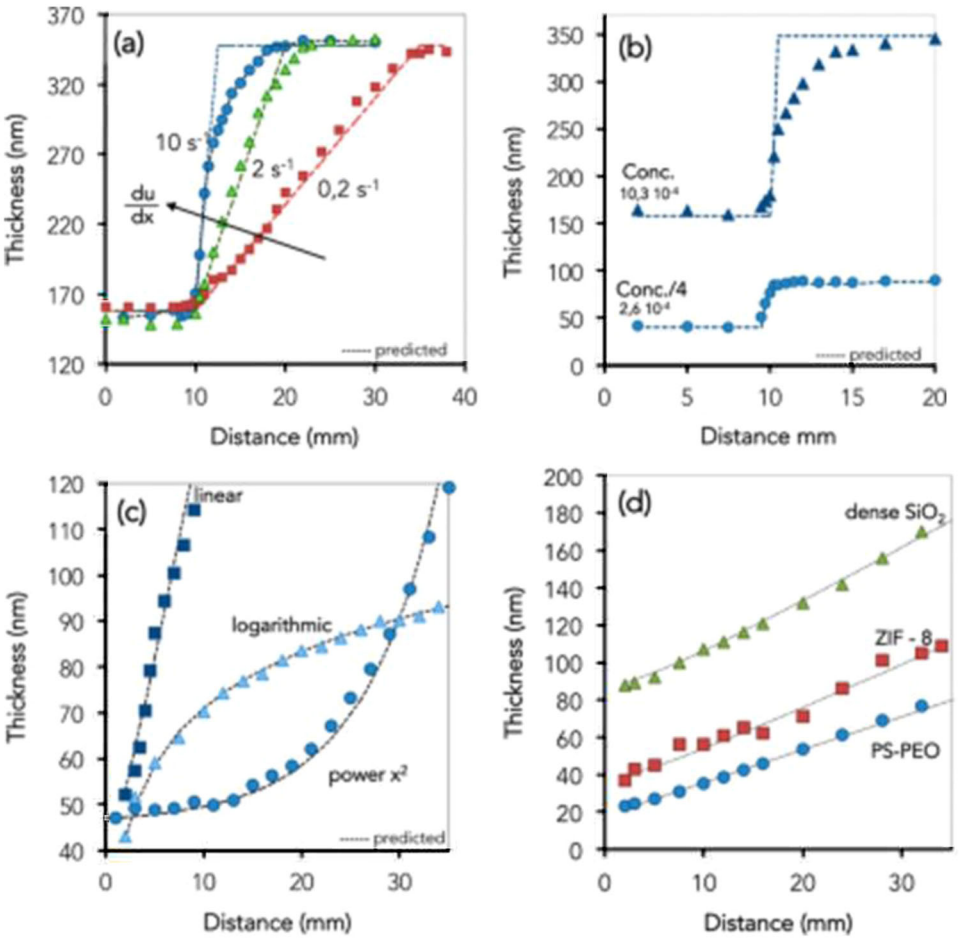

Fig. 5 **a** Plot of graded mesoporous titanium films thickness for different acceleration rates; **b** effect of the dilution: plot of the thickness of graded mesoporous titanium films from solution with two different concentrations and speed; **c** thickness of graded mesoporous titanium films for linear, logarithmic, or square power profiles; **d** plot of the thickness of linear graded films of different coating systems [22]. Copyright 2014, American Chemical Society

3.2 Sol–gel dip-coating

Sol–gel technique is one of the most commonly emerging chemical approach for textiles finishing, which is efficient, low cost, less chemical consumption, and excellent functionality [44]. The process of depositing zirconia coatings onto woven fabric via sol–gel process has been also investigated, where zirconia sol was synthesized using hydrothermal technique [45]. To improve the fracture resistance of fiber reinforced composites and modify fiber-matrix bonding conditions, tetragonal zirconia interfacial layer was introduced by sol–gel dip-coating for reinforced fiber [46].

During sol–gel process, the starting precursors compounds consist of metalloid element and various ligands, whereas silicon alkoxides and titanium alkoxides are the most common precursors. Dip-coating is a facile approach for the application of sol–gel in film disposition onto fibrous materials surface. For instance, anatase titanium coatings have been successfully fabricated by sol–gel dip-coating process on aluminium oxide fibers [47]. Moreover, a series of boron-doped silica sols were applied to wool fabric through the dip-coating sol–gel process to improve flame retardance and thermal stability [25]. Flax fibers were functionalized by grafting TiO_2 film via dip-coating process, which exhibited significant improvement in mechanical properties [26]. It should be noted that composites sol–gel has been an emerging finishing method for fibrous materials, such as SiO_2/TiO_2-doped cationic coating [48], hybrid SiO_2/HTEOS/CPTS sol [49], F/TiO_2 hybrid sol [50], and cationic SiO_2/TiO_2 hybrid sol for transfer printing [51]. Especially, cationic SiO_2/TiO_2 hybrid sol is synthesized and coated onto cellulose fabric surface, which could be used in the transfer printing of disperse dyes. The procedure of cellulose fabric modification and fabric transfer printing as shown in Fig. 7. Cellulose fabric was immersed into cationic SiO_2/TiO_2 hybrid sol at room temperature for 30 min and dried. Then red lump and pattern were printed to transfer paper through an inkjet printer, and then transferred to cellulose fabric to obtain the color pattern [51].

Compared with directly solution dip-coating, sol–gel-based dip-coating is a more complex dynamic process, which is closely time-dependent evaporation-induced concentration and viscosity gradients during sol–gel self-assembly. The coating solutions of sol–gel dip-coating for fibrous materials is always non-Newtonian fluids, solvent

Table 1 Summary of various dip-coating methods

Methods	Advantages	Disadvantages	Examples
Solution dipping	Easy operation, potential for scale-up production	Poor uniformity, relative weak bonding conditions	Potassium titanate whisker (PTW)-filled carbon fabric [23]; Carbon nanotubes (CNTs) coated cellulose fiber [24]
Sol–gel dip-coating	Efficient of fibrous materials functional finishing with oxide	Chemical reaction on fibrous surface	Wool fabric treated by boron-containing silica sols [25], TiO_2 thin film on natural cellulose fiber [26]
Spin-assisted	Uniformly deposited film, accelerate deposition	High demand of equipment	Dip-spin-coating for microstructured lithium-ion batteries [27]
Multi-layer dipping	Good uniformity, multi-layer structure coating	Relative low efficiency	Two-step dip-coating for solar cell electrodes[28], Single fiber-based supercapacitor [29]
Vacuum-assisted	A wide range of substrates, facilitate coating solution deposition	Complicated dip-coating devices	Vacuum-assisted dip-coating on Al_2O_3 hollow fiber [30], Graphene oxide-coated cotton fabric [31]
Photo-assisted	Benefit to improve the decomposition of coating precursors	Complex photo-chemically evaporation approach	Photo-assisted growth of silver nanoparticles [32]

evaporates, and the coating process simultaneously inducing a variation of viscosity, density, and surface tension, etc. Grosso et al. [16] reported that the phenomenon such as viscosity variation, evaporation cooling, chemical reaction, and thermal Marangoni flow may not have to be taken into account during sol–gel dip-coating process. Various experimental parameters are discussed together, and a semi-experimental equation has been established to characterize the deposited films on the surface of fibrous materials.

3.3 Spin-assisted dip-coating

Conventional solution dip-coating and sol–gel dip-coating process is based on the solid–liquid inherent interaction between surface tension and fibrous materials substrate. However, in spin-assisted dip-coating process, coating solution is scattered onto the center of a rotary table with fibrous materials. The film could be successfully deposited on the substrate under centripetal forces and evaporation conditions [52–54]. A typical spin-assisted coating device as shown in Fig. 8a, substrate was mounted in a Teflon holder and then rotated horizontally using a spinner [55]. Dip-coating followed by rapid spin drying is also an conventional form of spin-assisted dip-coating, the apparatus as shown in Fig. 8b. The dip-spin process was achieved by applying a voltage to the fan, and further dipping and spinning steps could be applied according to various substrate loading. Mathematical description of Newtonian fluid coating on rotating disk was developed for the production of television screens prepared by the rotational casting of a phosphor loaded slurry [27]. By considering centripetal and viscous forces acting at any point within the coating solution, the deposited film thickness, h (m), was established to be independent of the initial film thickness, h_0 (m), for long times and fast spin speeds [56]. The deposited film thickness could be calculated by the following equation:

$$h = \frac{1}{\omega}\sqrt{\frac{3\eta}{4\rho t}} \tag{6}$$

where ρ is the density (kg m^{-3}), and η is the viscosity g (Pa s), of the fluid, ω is the angular velocity of rotary disk (s^{-1}), and t is the spin time (s). Furthermore, hot spin-assisted dip-coating technique was developed by heating substrate to required temperature. During the spin-assisted process, large thermal mass of crucible molten glass produce a temperature gradient through the substrate, then the interfacial region between substrate and film reaches a temperature where the glass may flow [57]. In my opinions, this hot spin-assisted dip-coating method has the potential advantages in fiber reinforced composites. Especially, for the fabrication of thermoplastic composite reinforced with

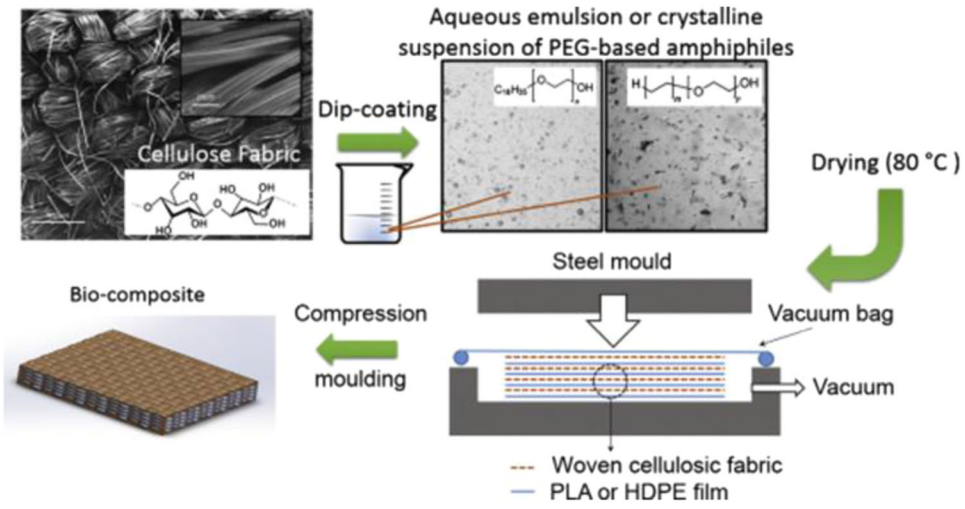

Fig. 6 Schematic representation of dip-coating for cellulose fabric and the fabrication procedure of fabric reinforced bio-composite via compression molding [35]. Copyright 2015, Elsevier

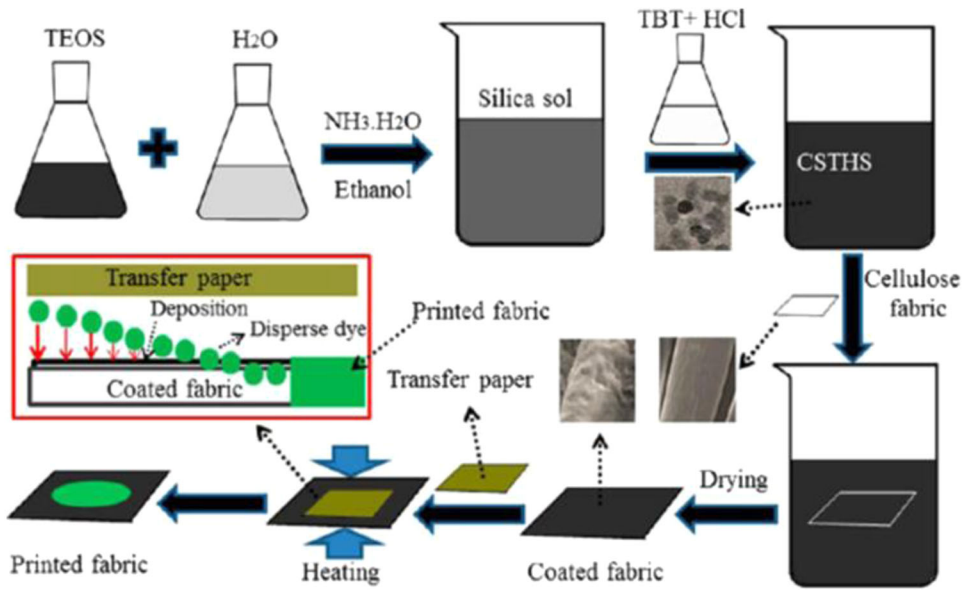

Fig. 7 Schematic of cationic SiO_2/TiO_2 hybrid sol preparation and transfer printing process [51]. Copyright 2013, American Chemical Society

fabric, where the fabric could be preheated by hot spin-assisted process to improve the interfacial interaction.

It has been demonstrated that the spin-assisted process utilizing centrifugal force, viscous force, air shear, and electrostatic interactions causes adsorption, which could facilitate the rearrangement of polymer chains when coating solution deposited onto substrate [58]. Despite the film-forming process assisted with spinning is much more time-saving than conventional dip-coating process, highly ordered internal structure could be obtained. Especially, it is feasible to predict and precisely control the thickness, even the architectural feature and surface roughness of deposited film could be well designed. Roberts et al. [27] described a new and economic route for the formation of three dimensional microstructured battery electrodes. The application process begins by dipping the substrate into a coating solution, and then followed by rapid spinning to obtain uniformly deposited film. In addition, titanium dioxide films were fabricated on the α-aluminium oxide substrates using the sol immersion and spin-coating process. The resulting titanium dioxide films exhibited more uniform titanium dioxide grains on the deposited film and increased photocatalytic activity [55]. It should be noted that the development of spin-assisted layer-by-layer assembly method [59] would broaden the horizon for spin-assisted dip-coating onto fibrous materials substrates. The researches [58, 60] indicated that the combination of layer-by-layer assembly and spin-coating is an efficient way to accelerate the film deposition process. Moreover, it has been indicated that coating solution concentration and spinning rate are the two

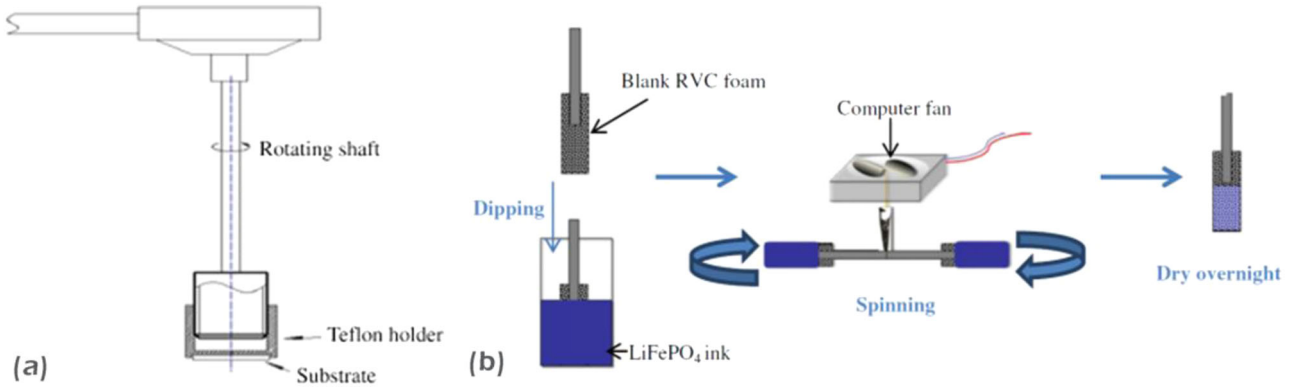

Fig. 8 Diagram of **a** sol–gel spin-coating device [55]; **b** dip-coating process followed by rapid spinning [27]. Copyright 2013, Elsevier

main parameters for deposited film thickness, and high stratified structure with well-defined layer could be obtained by spin-assisted layer-by-layer assembly [61]. The key technical points of spin-assisted layer-by-layer assembly could be applied to the dip-coating process, thus taking the potential advantages of spin-assisted technique, such as rapid film deposition, structure design, and dipping process control. The spin-assisted process should emphatically considering the intrinsic properties of fibrous materials, for instance, the porosity and flexibility, which would facilitate the adsorption and flow of coating solutions.

3.4 Multi-layered dip-coating

Multi-layered dip-coating was initially studied to improve the uniformity or increase the thickness of single dip-coating deposited film. The simple multi-layered dip-coating process as shown in Fig. 10a, b, coated fibrous materials were prepared via two-step dip-coating procedures. Fabrics were dipped into different coating solutions successively to achieve the functional complex of deposited layers. Compared with single dip-coating process to fabricate deposited film for fibrous materials substrates, the repetition of dip-coating is more efficient and applicable to produce multi-layer deposited film. For instance, transparent conductive indium tin oxide (ITO) film could be prepared on optical fiber through a multiple step dip-coating process [62, 63]. In details, the fiber was dipped into the ITO sol, then dried, annealed, cooled, and treated by ultrasonic wave. Steady multi-layer conductive ITO film-coated quartz optical fibers could be obtained by repeating the above-mentioned process. Figure 9a showed the schematic diagram of graphene oxide-coated carbon fabric by dip-coating, carbon fabrics are pulled out from suspension by from the graphene oxide suspension equivalent pulling forces. Surface morphology of original carbon fabric and coarse surface with different layered structures from graphene oxide sheets, as shown in Fig. 9b–f. It is obviously observed that the graphene oxide layers covered on the surfaces of the carbon fibers are increased with the increase of dip-coating cycles [33]. Dolay et al. [64] fabricated metal core piezoelectric fibers for structural sensing and driving properties through multi-layered dip-coating process. The results indicated that decreasing the slurry temperature during dipping process is suitable to reduce the number of dip-coating steps, and benefit to achieve high aspect ratio metal core piezoelectric fibers. In addition, multi-layers could be prepared by hybrid-coating solutions consist of different sized silica and polystyrene particles through multi-layered dip-coating process [65]. Pigmented multi-layer protective coatings was also prepared by repeatedly alternating a layer of resin deposited by dipping [66]. Furthermore, Pu et al. [28] developed a two-step dip-coating technique to prepare Ag nanowire networks onto polyethylene terephthalate (PET) substrates. The PET substrates were firstly immersed into Ag nanowire solutions and dried, afterwards, the substrates were tuned vertically to conduct the second-step dip coating. Thus the Ag nanowire networks-coated PET substrates with order-enhanced analogous crisscross arrangement was successfully prepared. It can be seen that the repeating of multi-layered dip-coating process could not only increase the thickness or improve the uniformity, but also manufacture the coatings with given functionality.

Compared with the repeated dip-coating process of single coating solutions, multi-layered dip-coating for different coating solutions show more advantages considering the synergistic effect of deposited layers. It should be noted that multi-layered dip-coating is different from layer-by-layer assembly, which is fabricated by alternately dipping a charged substrate into aqueous solutions of oppositely charged materials with intermediate steps of rinsing in water [59]. Multi-layered dip-coating of various coating solutions is mainly to achieve the functional superposition by several deposited film. A novel graphene coaxial fiber supercapacitor consist of wet-spinning core graphene fiber and facilely immersing coated graphene sheath could be

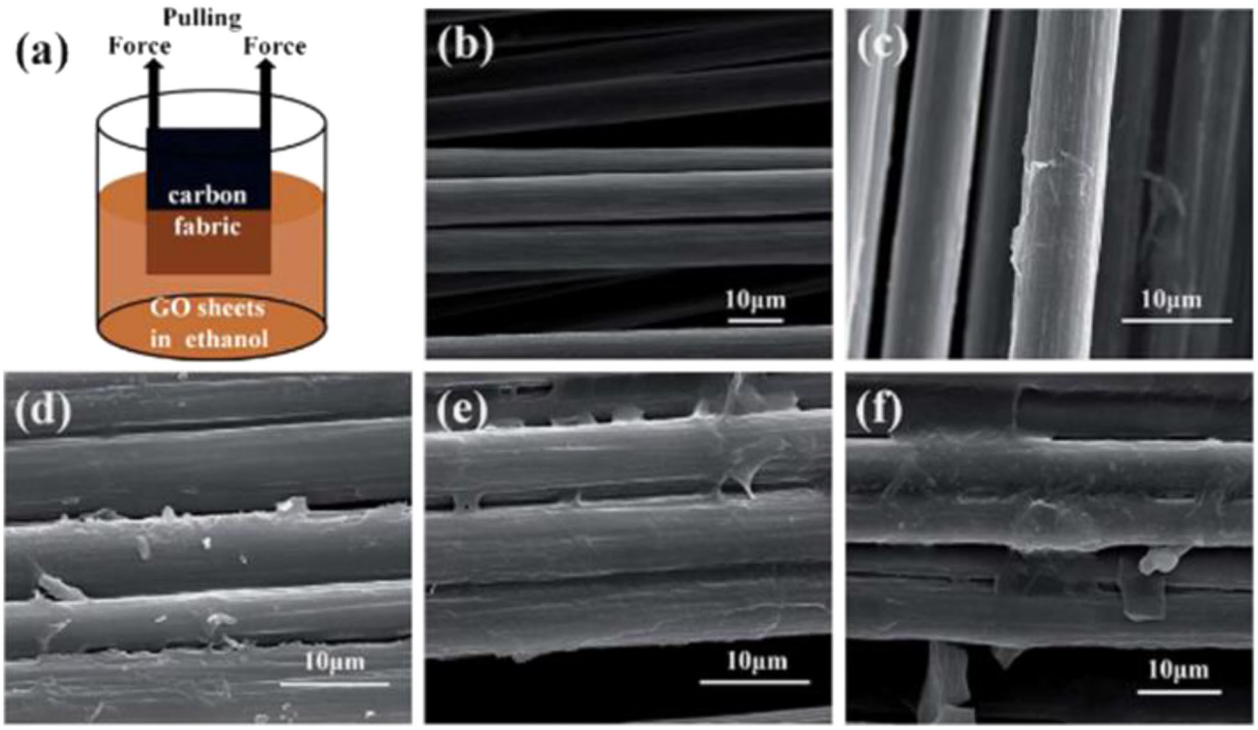

Fig. 9 **a** Schematic diagram of graphene oxide-coated carbon fabrics via dip-coating process; SEM images for **b** original carbon fiber, carbon fiber coated by the graphene oxide interlayers for **c** 5, **d** 10, **e**. 15, and **f**. 20 cycles, respectively [33]. Copyright 2014, Royal Society of Chemistry

successfully fabricated by multi-step dip-coating process. Graphene fiber was firstly dipped into polymer electrolyte gel, graphene oxide gel then reduction, and immersing into polymer electrolyte again, as shown in the schematic diagram of Fig. 10c [29]. The obtained cross-section structure of graphene coaxial structure with core fiber and cylinder sheath as two electrodes could be seen from Fig. 10d. The coating thickness and structure could be well controlled by changing the number of coating cycles and the concentration of various coating solutions [29]. The fabrication is facile and easy to achieve the multi-functional synergies of each deposited layer. And this multi-layer dip-coating process is benefit to broaden the applications of fibrous materials, such as in the fields of supercapacitor, lithium ion battery and electrode plate, etc.

3.5 Vacuum-assisted dip-coating

Vacuum-assisted dip-coating technique was recently developed to obtain a complete coverage of nanoparticles on the support substrate surface with minimum defects, including metallic and ceramic fiber, etc. Mesoporous α-alumina and Pd-α-alumina layers have been deposited on macroporous α-alumina hollow fibers by vacuum-assisted dip-coating technique. During dipping process, a vacuum is applied on the opposite side of the membrane to improve the absorption of coating solutions [30]. In addition, porous γ-alumina tube could be activated with palladium nuclei by dipping into chloroform solution of palladium acetate, followed by reduction with aqueous hydrazine at room temperature. Then coated with γ-alumina protecting layer by sequentially dipping, firing, and cooling. Finally, this tube was subjected to electroless plating by applying a vacuum-assisted process from the inner side of tube. The vacuum-assisted dip-coating process provide a new route for the fabrication of tubular membrane with a novel configuration [68]. Smith et al. [69] has developed a solvent-based fluid–liquid–solid approach for the growth of semiconductor nanowires. Flexible Ge nanowire fabric was made by vacuum-filtering a dilute dispersion of nanowires in chloroform. It has been reported that yttria-stabilized zirconia electrolyte membrane was deposited onto the outer surface of the presintered NiO-YSZ hollow fiber using a vacuum-assisted dip-coating technique. The anode fibers was firstly sealed at one end and then dipped into the suspension of yttria-stabilized zirconia [70]. Bazzarelli et al. [71] investigated the properties of styrene-butadiene-styrene triblock copolymer composites membranes, which prepared by vacuum-assisted solvent evaporation process. And the vacuum-assisted dip-coating produced coating layers was successfully applied on vinyl acetate comonomer hollow fibers. Nickel foam structure and PDMS were successfully

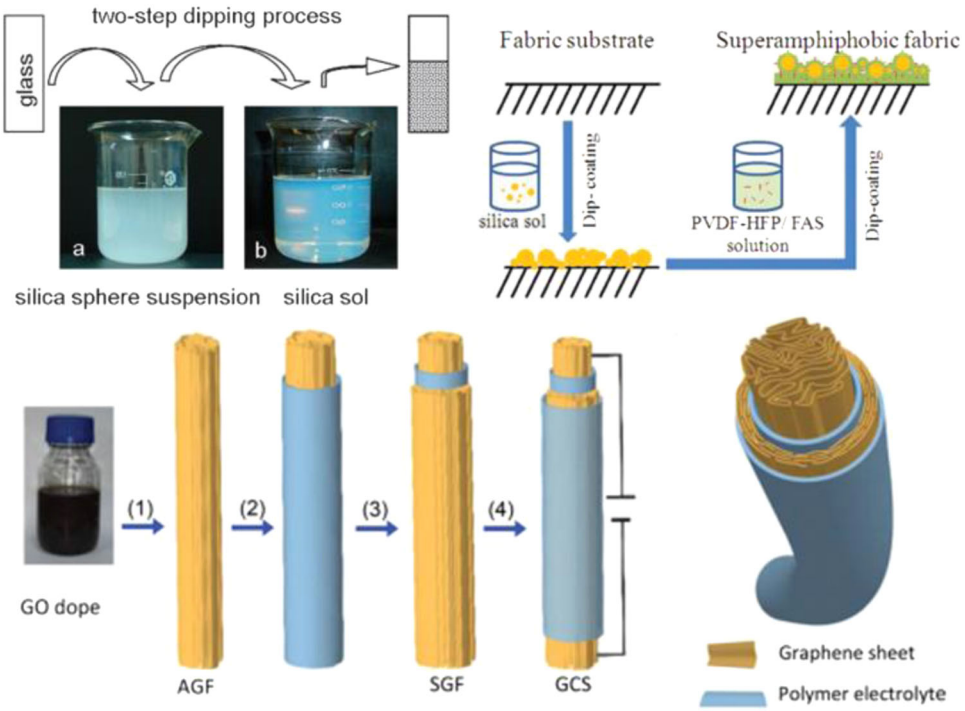

Fig. 10 **a**. Schematic of the two-step dipping process for silica microsphere suspension and silica sol [37]; **b**. two-step dip-coating procedures to prepare superamphiphobic fabrics [67]; **c** and **d** fabrication process and the cross-section structure of graphene coaxial fiber supercapacitor with a core and a cylinder sheath as the electrodes [29]. **a** Copyright 2011, Royal Society of Chemistry; .**b** copyright 2013, American Chemical Society; **c** and **d** copyright 2015, Royal Society of Chemistry

mimicked into free-standing three-dimensional graphene foam via facile vacuum-assisted dip-coating process. Vacuum infusion treatment graphene foam results in a resilient and flexible composite, which exhibited typical fracture behavior and controllable sensitivity for sensor applications [72].

To obtain uniform coatings of zeolite particles on the polymer-based fibrous supports, a vacuum-assisted dip-coating apparatus was set up as shown in Fig. 11a, the substrate to be coated was taped onto a fixed porous metal plate supported by a holder. In addition, the effects of coating dispersion concentration and particle size were studied. The results indicated that smaller particles were found to be more prone to cracking than larger particles, while smaller particles were advantageous to improve adhesion with substrate, obtain thinner thickness, and for tiny inter-particulate pore size [73]. Recently, Tang and coworkers [31] reported that vacuum-assisted dip-coating could be effectively fabricate graphene oxide nanosheet coated cotton fabric, the deposition process as shown in Fig. 11b. The fabrication process of cellulose-based composite via the combination of vacuum-assisted dip-coating and hot press could be seen from Fig. 11c. Compared with the most studied solution dip-coating and sol–gel dip-coating technique, vacuum-assisted dip-coating show unique advantage in more widely substrates, such as metallic, ceramic, and high performance polymer-based supports. Also it should be noted that vacuum assistant dip-coating technique is efficient to fabricate uniform coatings onto fibrous substrate.

3.6 Other modified dip-coating methods

Photo-assisted dip-coating technique is the process that the film fabricated under the auxiliary of photo conditions. For instance, mixed solution of zirconium-octylates and yttrium-octylates was dip-coated on a substrate and decomposed into yttria-stabilized zirconia thin films by heating under vacuum ultraviolet light irradiation [75]. The results indicated that active oxygen generated by the photo-assisted process is benefit to facilitate the decomposition of precursors. Calcined titania thin films was also immersing into methanolic solutions of silver nitrate with differing concentration to produce films with a variation in surface silver loadings, then the silver nitrate coated films were photo-irradiated to fabricate nanoparticulate silver [32]. Sliver surface loaded titanium oxide thin films were successfully fabricated by a modified spray-deposited method, followed by dipping into methanolic solutions of silver nitrate and photo-chemically evaporation approach, as shown in Fig. 12a. Methanol is beneficial to prevent the recombination processes of electron-hole pairs generated during irradiation, thus driving the reduction of surface absorbed silver(I) ions [76]. Compared with conventional dip-coating process under the self-assembly evaporation of coating solutions, photo-assisted growth of deposited film is an efficient approach considering the role of photo irradiation.

Inverse dip-coating technique that consists of dip coating for inner wall of a preform with a liquid sol of silica and zirconia precursors has been developed by Brasse et al. [77],

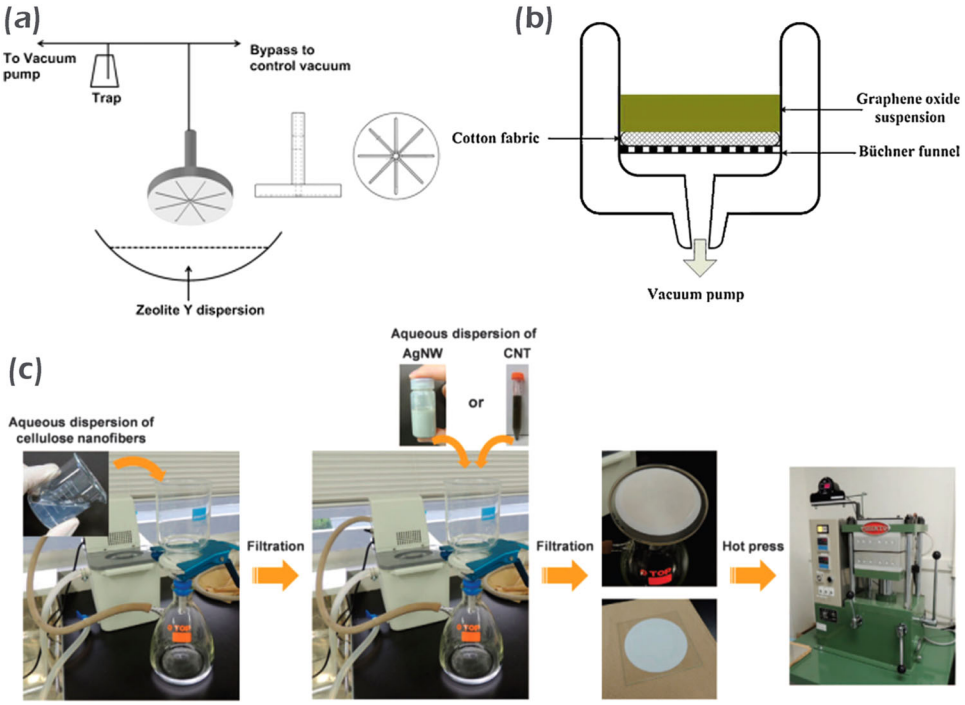

Fig. 11 **a** Schematic of the vacuum-assisted dip-coating set up [73]; **b** graphene oxide-coated cotton fabric fabricated by vacuum filtration coating [31]; **c** vacuum filtration coating of cellulose-based nanopaper [74]. **a** and **b** copyright 2015, Elsevier; **c** copyright 2014, Nature Publishing Group

which is suitable for the preparation of nanostructured optical fibers. However, the obtained nanostructured deposition films by inverse dip-coating is limited, template-assisted dip-coating techniques show unique advantages in fabricating thin films with ordered porosity. Dewalque et al. [78] investigated the effects of long-range order, percentage of porosity, pore size and pores connectivity on the deposited film organization, and porosity. And the micro-holes could be significantly increased by controlling the solvent drying process [79]. Template-assisted dip-coating technique is valid to shorten the traditional calcinations process for micron-scale thin films preparation exhibiting high porosity.

Dip-coating process also facilitates the ordered arrangement of one-dimensional nanotubes and nanowires. Stone et al. [80] studied the effect between long axis-oriented direction of the dipping fibers and the direction of extraction, and the withdrawal of fiber from CNTs provides essential force for the orientation of CNTs along fiber surface. The results indicated that shear forces accompanying withdrawal of the fiber are greater than any randomizing influences of Brownian motion, and CNTs could be effectively aligned by this dip-coating steps. Yang et al. [81] also reported that the dip-coating method could assemble nanowires directly from coating solutions; thus the processing steps required for making one-dimensional nanowire-based devices could be significantly decreased. Arrays of aligned nanowires for large areas was successfully achieved by programming the stick-slip motion of solvent contact line during dip-coating process. Based on the

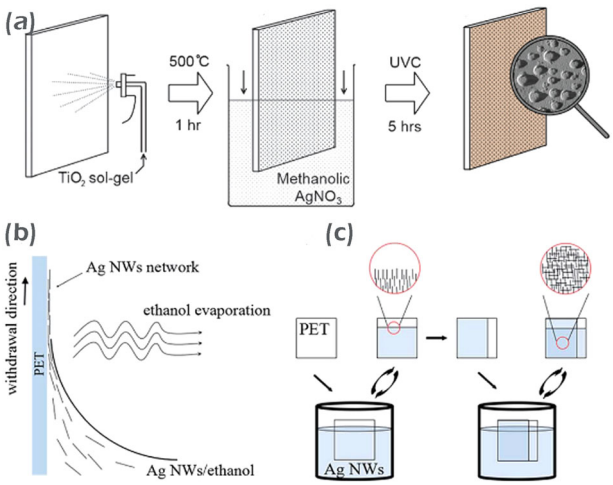

Fig. 12 **a** Step-wise illustration depicting the fabrication of the silver loaded anatase thin films via photo-assisted dip-coating [76]; **b** schematic diagram of nanowire assembly in the dip-coating process; and **c** two-step dip-coating process for order-enhanced silver nanowire networks [28]. **a**. Copyright 2011, Royal Society of Chemistry; **b** and **c** copyright 2015, Royal Society of Chemistry

academic theory that isotropic one-dimensional nanowires aqueous solution were ordered or partially aligned toward anisotropic phase by capillary force along the contact line of air–liquid–solid interface. Controllable dip-coating process to prepare silver nanowires networks on PET fibrous substrates as illustrated in Fig. 12c. Silver nanowires adhere to the substrate and orient parallel to movement direction due

to capillary force, which could be seen from Fig. 12b [28]. The results indicated that perpendicularly crossing networks was successfully fabricated just by conducting the dipping direction of two-step dip-coating process. Thus it might be concluded that the dispersion of one-dimensional materials could be readily used for fibrous surface deposition to achieve controlled arrangement of the film via the stick-slip patterning technique.

4 Functional fibrous materials fabricated by dip-coating

The initial purpose of dip-coating for fibrous materials are mainly to increase the mechanical properties, abrasive resistance, spinnability, and weavability, however, which are not the focus of this section. For fiber reinforced composites, dip-coating is also an efficient approach for interfacial region modification, thus improve the interfacial strength and bonding conditions of composites [35, 45, 82, 83]. Recently, the functional applications of fibrous materials via dip-coating have been explored. Compared with the mostly studied functionalization approach for fibrous materials, such as graft modification, surface polymerization, magnetron sputtering, and vapor deposition, dip-coating is convenient for the large-scale fabrication of deposited films. In general, the deposited films prepared by aqueous solutions or sol–gel dip-coating exhibited excellent stability considering the penetration effects between coating solutions and fibrous substrates. The coating solutions could consist of multi-components to achieve the integration of multiple functions for fibrous materials. In this section, self-cleaning, oil-water separation, electrical conductivity, and energy applications of dip-coating fibrous materials are described and reviewed.

4.1 Self-cleaning fibrous materials

The self-cleaning surface of fibrous materials could be obtained both by hydrophobic and hydrophilic effects. Hydrophobic surfaces, which have high contact angles, could effectively protect against pollutants and dust during the usage of fibrous products. While for hydrophilic surfaces, the self-cleaning is based on the photocatalytic effect. When stains and pollutants are stuck on the surface of fibrous materials, which could be chemically decomposed by the photocatalytic reactions, the mechanism as shown in Fig. 13a. With the increasing demand for entire eco-friendly lifetime of industrial products, self-cleaning fibrous materials have large potential market globally considering the unique advantage of reduced water consumption during textiles laundering and care. Considering the unique advantages of dip-coating in surface modification, it is promising in the applications of self-cleaning fibrous materials.

Among various photocatalytic for self-cleaning textiles, titanium oxide is the mostly studied due to the relative high catalytic activity and stability. Velasco and coworkers [85] reported that the formation of polar functional groups such as carboxyl and aldehyde, which activated on fabric surface thus promote a stronger adhesion with titanium oxide. The reasons could be attributed to the binding of the suspended and positively charged titanium oxide particles onto the fibrous materials surfaces during dip-coating preparations. The effects of titanium oxide-coated self-cleaning cotton fabric for the degradation of coffee stains as shown in Fig. 13b, c [84]. It can be observed that the stains gradually fade away under solar light irradiation. The influence of dip-coating temperature on the titanium particle size distribution and average particle size for deposited coatings has been investigated. The results are benefit to produce variable-sized nanoparticles-coated cotton fabrics for controllable self-cleaning properties [86]. Silver and zirconium co-doped and mono-doped titania oxide were also coated on cellulosic fibrous materials via sol–gel dip-coating method. The results showed that the modification of titanium oxide by co-doping is an effective technique for increasing the photocatalytic activity, which could be attributed to the synergistic action both the structural and the electronic properties of the photoactive anatase phase [87, 88]. Apart from titanium oxide, nanometric thin films were also prepared by dip-coating and inkjet printing ZnO nanosheets. The side-by-side aligned ZnO nanosheets on the substrate resulted in thin transparent, oriented zinc oxide surfaces with the high-energy {001} toward high photocatalytic activity [9].

The photocatalytic self-cleaning properties of titanium oxide-based nanocomposites for fibrous materials have been investigated by dip-coating approaches. It was shown that a TiO_2-SiO_2 composites photocatalysis could be produced at temperatures of 100 °C with good photo-activity on non-heat resistant materials. The mixed titanium oxide and silica oxide colloids well deposited on cotton fabrics surface during the dip-coating process and subsequent thermal treatment, which produced organized structure with highly dispersed titanium oxide particles surrounded by amorphous silica [89]. In addition, Xin et al. [90] prepared spherical TiO_2/SiO_2 nanocomposites-coated cotton fabrics via facile dip-coating methods, and the results indicated that TiO_2/SiO_2 hybrid coatings exhibited better photocatalytic self-cleaning activity than pristine titanium oxide-coated cotton textiles. Furthermore, a durable layer of porous Au/TiO_2/SiO_2 nanocrystallites was presented to enhance the visible light self-cleaning performance. This visible light-driven photocatalytic enhancement treatment for flexible fibrous materials with a high potential for commercialization in self-cleaning textiles [91]. These photo-catalysis-

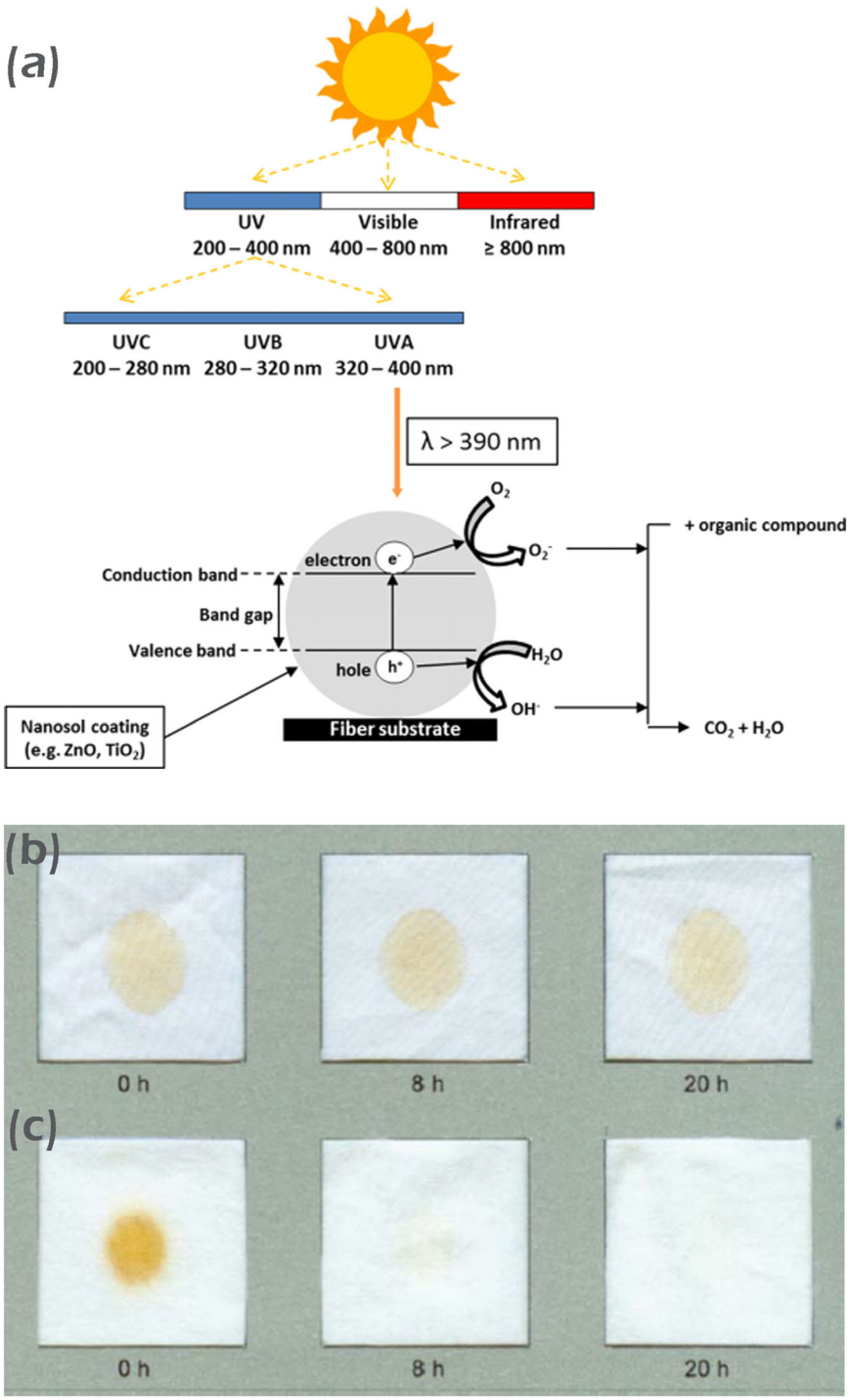

Fig.13 **a**. Photocatalytic mechanism of self-cleaning nanosol-coated fibrous materials [44]; Degradation of white cotton samples stained with a coffee stain on pristine cotton **b** and titania coated white cotton fabrics **c**, after different of solar light irradiation [84]. **a** Copyright 2016, Springer; **b** and **c** copyright 2006, Royal Society of Chemistry

coated cotton textiles possess significant self-cleaning properties, such as bactericidal activity, colorant stain decomposition, and degradation of red wine and coffee stains.

Surface roughness has also been shown to be a key approach in generating self-cleaning properties. Inspired by the natural lotus effect, various bio-mimetic hydrophobic surface have been fabricated for fibrous materials substrate. For instance, silver nanowires were synthesized and coated onto commercial cotton fibers through a simple dip-coating process. The obtained cotton fabric showed excellent hydrophobicity and UV-blocking ability [92]. The hydrophobic effect as shown in Fig. 14a–d, which water droplet could be enduringly non-wetting on the fibrous substrate. The penetrating capability of one-dimensional nanoscale materials is beneficial in physically attaching onto the

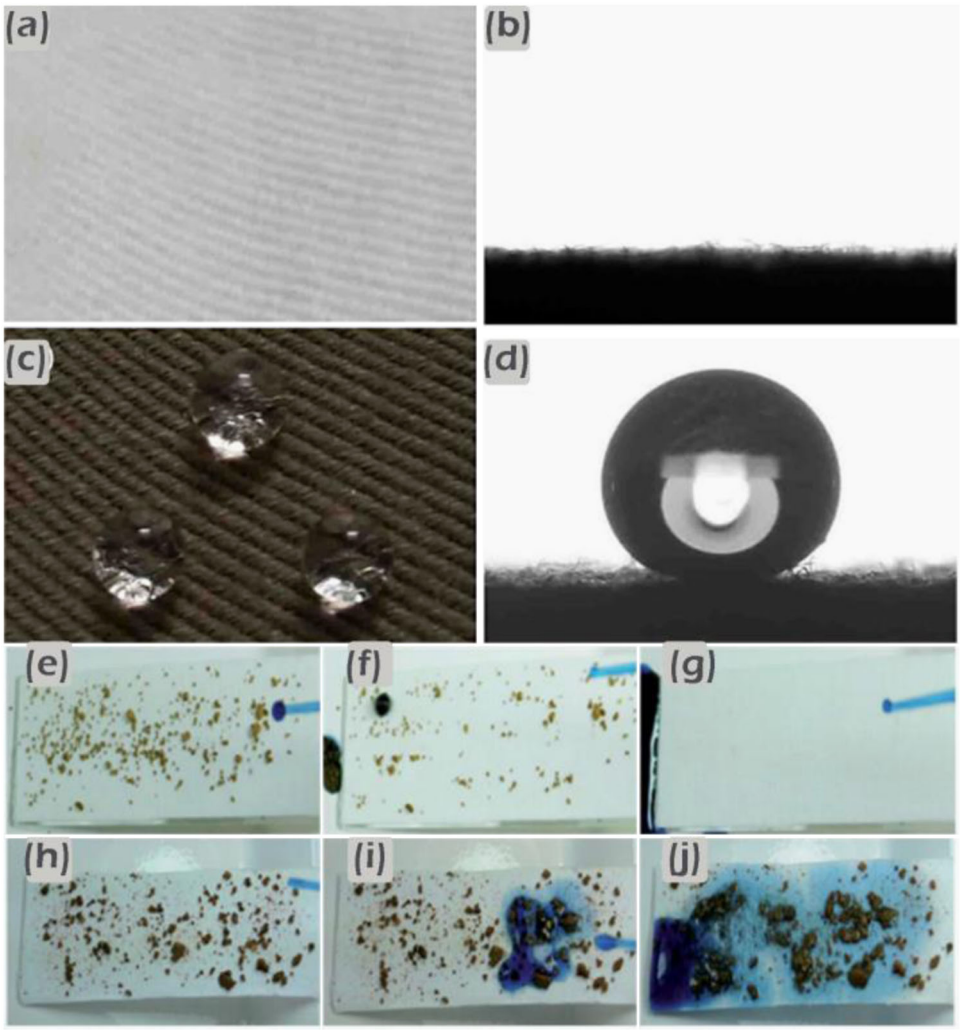

Fig.14 Water droplets sitting on pristine cotton fabric (**a** and **b**), and Danasylan®F 8815 coated AgNWs-loaded fabric (**c** and **d**), goniometer photographs for 5-μL droplets as shown in (**d**) [92]; Still frames taken from videos showing droplets of water on the dust contaminated fabrics, (**e–g**) superhydrophobic coated fabric, and (**h–j**) uncoated cotton fabric [93]. (**a–d**) copyright 2015, Elsevier; (**e–j**) copyright 2015, Royal Society of Chemistry

fibrous surface. CNTs network armors have also been fabricated on the surface of cotton fibers using a simple solution dip-coating method. The modified cotton textiles exhibited super water repellent properties simultaneously with enhanced mechanical behavior, flame retardancy, and improved UV-blocking properties. Especially, the exceptional electronic properties of functionalized cotton fibers will find a variety of potential applications in high performance fabrics and smart textiles [94]. Furthermore, titanium oxide hybrid sol was synthesized with tetrabutyl titanate and a fluoride silane coupling agent, thus enabling preparation of a functional surface with alterable superhydrophobic and superhydrophilic wettability under UV-switchable conditions. To improve the switchable sensitivity between superhydrophobicity and superhydrophilicity, various ions were doped and the dynamically modifiable wettability was investigated in detail [95]. To investigate the self-cleaning ability, Zeng and coworker [93] placed dust on the coated fabrics and then cleaned the stained surface by purging with water. As shown in Figs. 14e–g, the dust could be easily taken away by the moving water droplet, thus completely clean the surface [93]. However, the dust on the uncoated cotton fabric was hard to clean in a similar method as shown in Figs. 14h–j. This indicates that the self-cleaning properties of treated fabric could be achieved by lotus leaves of hydrophobic effects. Therefore, it could be seen that conventional dip-coating method is beneficial for the fabrication of uniform self-cleaning films onto fibrous surface, both from the aspects of photocatalytic and superhydrophobic. The enhanced self-cleaning properties could be achieved by the modified dipping and coating process, and various doped solution components for the functionalization of deposited films. In summary, dip-coating is a promising method to fabricate self-cleaning fibrous materials and textiles.

4.2 Oil–Water Separation

Oil–water separation is an increasing important area both for scientific research and industrial applications

considering that oily wastewater has become the most common pollutant all over the world [96]. To meet the growing demand of large-scale oil–water separation materials, low cost and good reusability processed by easy techniques are necessary. Compared with traditional technology, dip-coating treatment of fibrous materials for oil–water separation is a promising field, and more research needs to be done in this area to explore the potential advantages of dip-coating for oil–water separation fibrous materials. The oil–water separation composites made from fibrous materials, was usually thought to have good mechanical stability and flexibility than free-standing separation films.

Dip-coating is a facile but versatile approach that could easily achieve surface morphology adjustment and special coating composition required for controllable wetting behaviors. Yoon and coworkers prepared a simple, low cost fibrous composite membrane suitable for gravity-driven oil–water separation and water purification. The facile dip-coating approach is readily usable for industrial mass production [97]. Para-aminobenzoate alumoxane, boehmite-epoxide, and polycitrate alumoxane coated on the Kevlar fabric according to a three-step dip-coating process for oil separation from oily water emulsions have also been reported [98]. Nanoparticles-based inorganic/organic hybrid-coating solutions for oil–water separation fibrous materials has been investigated, which could integrate the adhesive of organic solutions and functionalization of nanoparticles. It has been reported that nanocomposite coating solutions is a promising approach for preparing durable oil–water separation fibrous materials by dip-coating [99]. The nanocomposites help to increase the superhydrophobicity, superoleophilicity, mechanical, and chemical stabilities. For instance, hydrophobic filtration polyester fabric was fabricated through dip-coating in the mixture solutions of poly(dimethyl siloxanes) (PDMS) and silica toluene dispersion [100]. Typical fibrous materials, including fabric and sponge were dipped into the silica nanoparticles-based polyfluorowax hydrophobic hybrid solutions to obtain superhydrophobic surface. The results indicated that the resulting superhydrophobic fibrous materials could be used as functional separation membranes to effectively separate oil from oily water mixed solutions [101]. Cao and coworkers [102] prepared films with excellent superhydrophilic and under-water superoleophobic, which could separate a range of different oil/water mixtures, such as immiscible oil/water mixtures and surfactant stabilized emulsions. This method can be applied on organic and inorganic substrates and used in preparing large-scale product, which has excellent potential in fibrous materials-based oil/water separation applications.

The mechanism of fibrous materials for oil–water separation was schematically explained by Fig. 15. When a water droplet dropped onto the superhydrophobic filtration fabric (SFF), it was thought to be in Cassie state, which could easily move away due to the superhydrophobic effects, as shown in Fig. 15a. However, oil droplet could quickly permeate through the fabric, as illustrated in Fig. 15b. During separation process, the surface was wetting by oil, thus the surface structure and composition had changed, which was shown in Fig. 15c [100]. The roughs structure of fibrous surface was filled with oil, thus when a water droplet was dropped, it preferred to keep in Wenzel state with low water contact angle [100]. It should be noted that the surface wetting by oil became easily flow for water and effectively separate water from oil, which could be attributed to the low resistance between water and oil wetting surface. The practical separation process as shown in Figs. 16a–e, where water was efficiently separate from n-hexane via a facile method. It was obvious that the SFF performed both superhydrophobicity and superoleophilicity, and n-hexane quickly permeated through the surface by gravity, while the blue water was flowed away into another beaker.

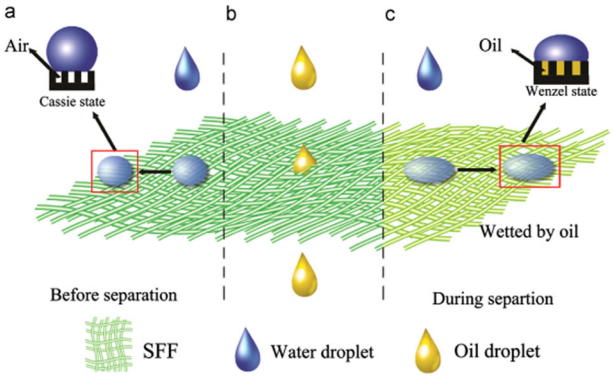

Fig. 15 Schematic diagram of the oil–water separation mechanism [100]. Copyright 2014, Elsevier

It has been reported that the low surface free energy of polybenzoxazine and photocatalytic-induced self-cleaning property of titanium dioxide could be well integrated. And the nanocomposites modified polyester non-woven fabrics were prepared through simple solution dip-coating and thermal curing approaches. The durable hydrophobic and oleophilic of coated fabric exhibited high separation efficiency just driven by intrinsic gravity, which could purify wastewater that contains soluble dyes and shed light in promising oil/water separation applications [103]. The alterable superhydrophobic and superhydrophilic wettability of fabric substrates decorated with ion-titanium coating as shown in Fig. 16f, the wettability of fibrous surface could be effectively converted under UV radiation and dark storage. Kong and coworkers fabricated self-adaptive wettability surface on fibrous materials through a simple one-step dipping coating treatment with titania sol–

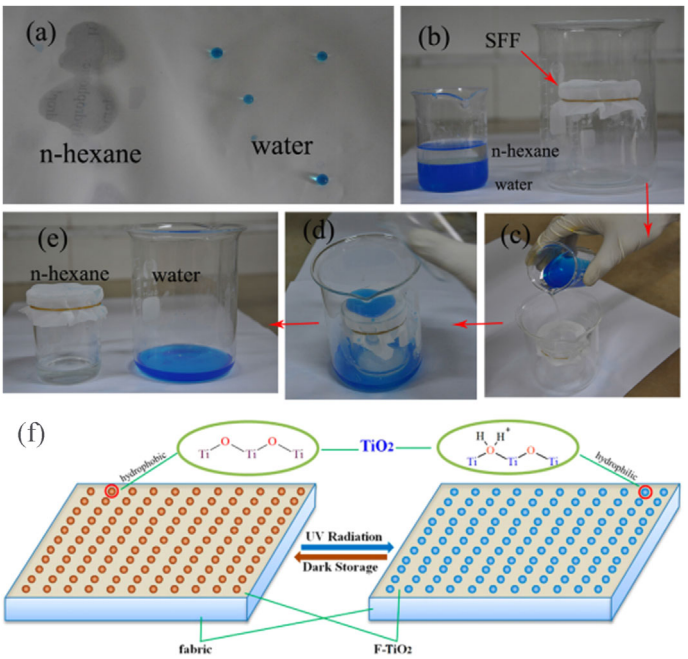

Fig. 16 **a–e** The process of separation of water and oil [100]; **f** alterable wettability between superhydrophobic and superhydrophilic under UV radiation [95]. **a–e** Copyright 2014, Elsevier; **f** copyright 2014, American Chemical Society

gel, the prepared fabric with one side superhydrophilic and another side hydrophobic properties, as shown in Fig. 17 [104]. In addition, switchable wettability surface was fabricated by spray-assisted dip-coating hydrophobic ZnO nanoparticles and waterborne polyurethane mixtures on stainless steel mesh. The results indicated that reversible transition between superhydrophobicity and superhydrophilicity could be rapidly realized by UV illumination and heat treatment alternately, which allows to change the mode of oil/water separation from oil-removing to water-removing [105]. Lin and coworkers [106] reported that silica nanoparticles and heptadecafluorononanoic acid-modified titanium sol-coated polyester fabric and polyurethane sponge via dip-coating approach, could alternatively turns superhydrophilic and superoleophobic upon ammonia exposure. This controllable wettability is promising in the application of selective removal of water from bulk oil and the design of smart interfacial materials. Therefore, as can be seen from the above-mentioned, dip-coating process could not only given the oil–water separation properties, but also it is feasible to achieve the multi-functionalization and intellectualization of coated fibrous materials.

4.3 Electrical conductive fibrous materials

Electrically conductive fibrous materials have various potential applications such as static charge dissipation, electromagnetic frequency shielding, health monitoring, battery devices, smart clothing, and even in tissue engineering, etc. Dip-coating is an emerging facile approach for the fabrication of electronic fibrous materials. Various fibrous materials could be taken as the substrate, and alternative coatings to achieve electrical conductivity have been proposed such as conductive polymers, metallics, and carbon materials. It has been reported that nylon, polyester, and cotton threads can be made conductive by dip-coating into synthesized silver nanowire solutions, thus deposited random networks onto the surfaces. The current-voltage curves and practical effects of nylon thread-coated nanowire densities to power and light-emitting diode as shown in Figs. 18a–b [107]. Carbon-based electrically conducting nanofillers, such as liquid exfoliated graphite, nano graphite, carbon nano fibers, and carbon nanotubes were also used to induce electrical conductivity in thermoplastic polyurethane matrix. The nanocomposites is suitable for development of electrical conductive coated fibrous materials [109]. Graphite-based coatings were fabricated and directly applied onto the surface of a paper made of recycled fibers to impart electrical conductive properties. In order to attain the graphite suspensions with high solid content and good dispersion, sodium dodecyl sulfate was introduced as dispersion agent [110]. Considering the excellent electrical properties of graphene nanoribbon, which was prepared and was coated to the cotton fabric using a wet coating approach recently, as shown in Fig. 18c. It was shown from the results that the graphene nanoribbons were uniformly distributed on the surface of the cotton fibers and interacted with the cotton fibers through hydrogen interactions. The thermal stability and electrical conductivity of the cotton fabric were simultaneously improved significantly [108].

The applications of electrical conductive fibrous materials have been investigated. Taking the advantages of dip-coating, electrical conductive fibrous materials shed light for potential fiber reinforced composites applications. For instance, carbon fibers were directly immersed in a stable graphene nanoplatelets suspension, and carbon fibers/epoxy composites were manufactured by a prepreg and lay-up method. The results indicated that the mechanical properties and electrical conductivity of the composites were improved [111]. Electrical conductive polypyrrole was also synthesized through dip-coating and in-situ polymerization process, and electric pulse-stimulated fibroblasts was investigated [112]. It has been demonstrated that graphene layers could be well assembled on surface of highly porous polyurethane foam to fabricate electrical conducting composites with excellent compression [113]. Highly stretchable conductive fibers could also be prepared by dipping poly(m-phenylene isophthalamide) fibers into the CNTs aqueous solutions. And annealing treatment was operated to increase the interaction between the CNTs and fiber surface. The simultaneously stretchability and electrical conductivity suggest the great potential in constructing advanced stretchable conductive electronics [114]. Koga and coworkers [74] fabricated highly transparent conductive networks on a cellulose nanofiber paper. Uniform coating of the conductive silver nanowires and CNTs, is achieved by simple dipping and filtration of aqueous dispersion through the cellulose nanopaper. The optical photographs and relative resistance values of coated nanopaper and PET film as shown in Fig. 19 [74]. It should be noted that compared with conventional textiles, cellulose nanofiber paper has the advantage that acts as both filter and transparent flexible substrate during the coating process. The electro-

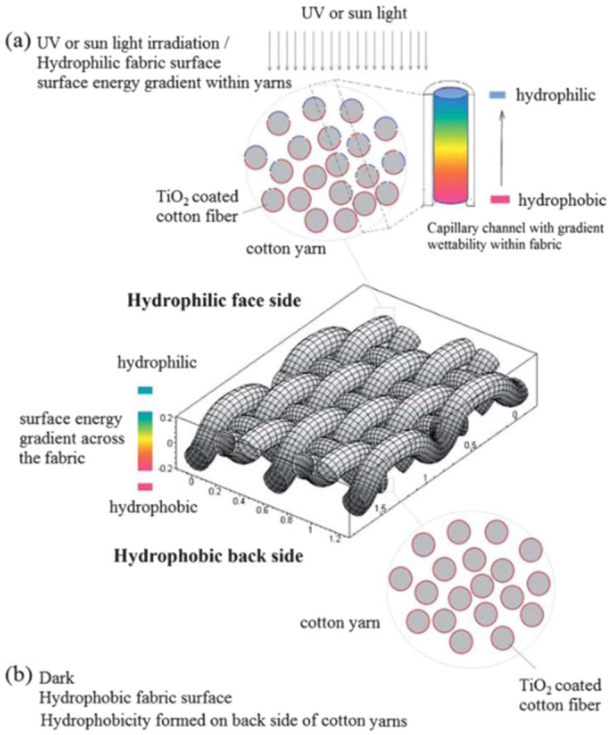

Fig. 17 Photo-induced superhydrophilicity of titanium oxide-coated textiles: capillary channels with gradient wettability formed within the fibrous matrix under irradiation and dark conditions [104]

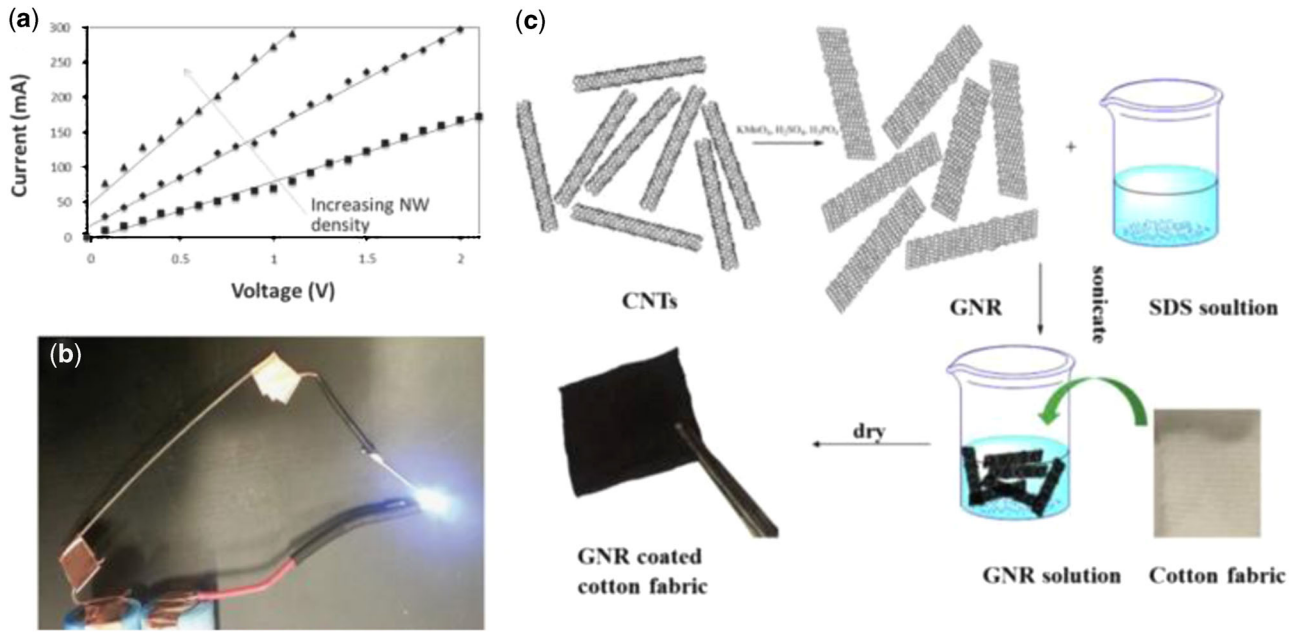

Fig. 18 **a** Current-voltage curves of nylon thread coated with different nanowire densities and **b** nanowire-coated nylon thread to power and light-emitting diode [107]; **c** schematic illustration of graphene nanoribbon-coated cotton fabric [108]. **a** and **b** copyright 2015, Royal Society of Chemistry; **c** copyright 2015, Elsevier

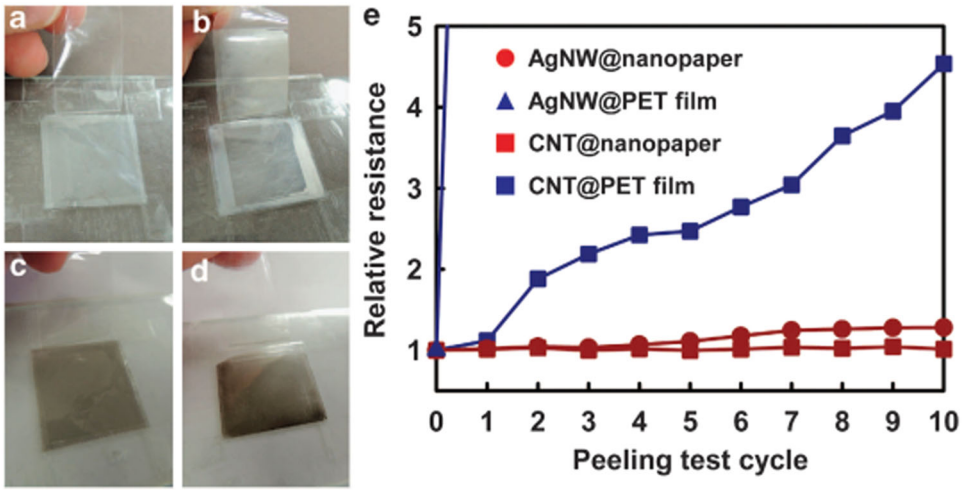

Fig. 19 Optical photographs of **a** AgNW@nanopaper, **b** AgNW@PET film, **c** CNT@nanopaper, and **d** CNT@PET film after the peeling test; **e** relative resistance values of AgNW and CNT coated nanopaper and PET film, respectively [74]. Copyright 2014, Nature Publishing Group

mechanical properties of Ag-coated polyether ether ketone filament show the potential advantages for structural health monitoring. Especially, Ag-coated polyether ether ketone filament yarns has good machinability for fiber reinforced thermoplastic composites [115]. Fibrous materials not only could be fabricated by facile dip-coating process, but also show excellent electrical conductivity. Low cost, flexible and renewable fibrous materials using dip-coating fabrication methods have attracted much attention recently as complement for textiles electronics. Much future investigation will facilitate the development of dip-coating for electrical conductive fibrous materials forwards.

4.4 Fibrous materials for energy storage

Fibrous materials energy storage systems are the foundation of fabricating smart textiles, in which fibrous materials directly serve as electrical energy storage devices. Compared with the most studied metallic and ceramic energy storage devices, the large surface area of textiles could also increase the energy storage capacity. Currently, the development of fibrous materials-based energy storage devices could be mainly categorized into three classes: (1) coated energy storage textiles, (2) fiber and yarn electrodes, and (3) custom woven and knitted fabrics [116]. Coated fibrous materials are the mostly studied and extensively used textiles energy storage devices, and dip-coating is efficient in incorporating active electrode materials into the surface of fibrous materials. Cui and coworkers firstly assembled CNTs onto cotton fabrics with simple dipping and drying approach [117]. It was reported that the excellent energy storage performance reached as high as 480 mF cm^{-2} for testing at 1 mA cm^{-2}, resulting in 120 F g^{-1} with a mass loading of 8 mg cm^{-2}. The prepared textiles energy storage devices show outstanding flexibility, stretchability, strong adhesion between the CNTs and the textiles substrates. Hybrid graphene/MnO_2 nanostructures-based energy textiles as electro-chemical capacitors electrode were also prepared by solution-based dipping process. The textiles energy devices exhibit maximum power density of 110 kW kg^{-1}, an energy density of 12.5 Wh kg^{-1}, and excellent cycling performance of about 95 % capacitance retention over 5000 cycles, which offer great potential for large-scale textiles energy storage devices production [118]. The preparation of fabric electrode by dipping the non-woven cloth into a dispersion of CNTs and subsequent MnO_2 electrodeposition was also reported [119].

Flexible supercapacitor could be also assembled by depositing single-walled CNTs and conductive polyaniline nanowire array composites on non-woven wiper cloth. Non-woven wiper cloth is firstly dipped into single-walled CNTs ink, then polyaniline nanowire arrays are grown onto the surface of CNTs/cloth composite through dilute polymerization to obtain the flexible textiles electrode, as shown in Fig. 21a [120]. Compared with traditional gold and stainless steel substrates, fibrous materials-based substrate with large surface area which not only acts as an interior electrolyte reservoir, but also could be diffused into an integrated energy storage system. Gui and coworkers [121] fabricated natural fiber-based supercapacitor via dip-coating and electro-chemical deposition methods, the schematic illustration as shown in Fig. 20. It demonstrated the merits of cellulose fibers as substrates for supercapacitor electrodes, in which the water-swelling effect of the cellulose fibers can absorb electrolyte, and the fibrous internal structure could provide channels for ions to diffuse to the electro-chemical energy storage devices [121].

Compared with supercapacitor, fibrous-based batteries are more challenging to integrate structurally complex batteries into flexible fibrous materials. Considering that

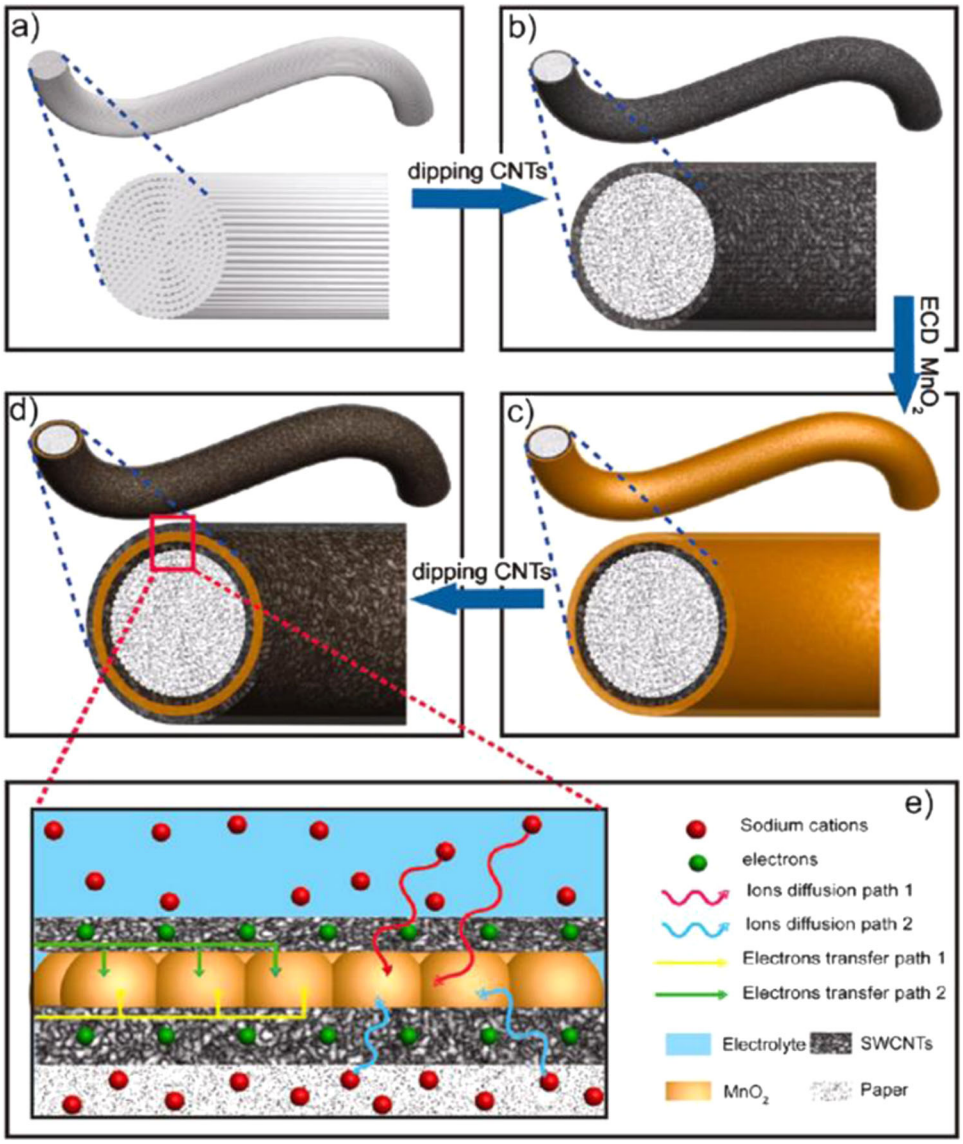

Fig. 20 Schematic illustration of natural cellulose fiber-based supercapacitor: **a–d** carbon nanotubes dip-coating and followed electrodeposition of MnO2, carbon nanotubes dip-coating again. **e** Magnification of the square area to depict the dual electron charge transfer and ion diffusion paths in the supercapacitor [121]. Copyright 2013, American Chemical Society

batteries always contain electrodes that are sensitive to water and oxygen, fibrous base batteries must be sealed inside without moisture penetrability [122]. It has been reported that lithium-ion textile batteries could be prepared by dipping into CNTs ink solutions, and dried in a vacuum oven. In the following, battery materials was incorporarted to prepare conductive textiles, which could be used as energy storage substrates. The results indicated that stable potential range of such conductive textiles inorganic electrolyte was achieved, and effectively working Li-ion battery under mass loading of 168 mg cm^{-2}, which are 8–12 times higher than conventional metal collector. In addition, such a fibrous material-based lithium-ion battery shows outstanding performance in capacity retention during cycling and little self-discharge [123]. With similar methods, hierarchical $ZnCo_2O_4$ nanowires arrays/carbon cloth and fibrous-based battery rechargeable by solar energy exhibiting high capacity, excellent cycling performance, and good rate capability have been successfully fabricated [124, 125]. Recently, it has been reported that carbon fiber with SnO_2 nanotubes networks coating were successfully fabricated by a simple dip-coating process and subsequent chemical vapor deposition growth approach, as shown in Fig. 21b. The as-prepared material, which could worked as a binder-free anode for lithium ion battery, delivers a reversible capacity of 653 mAh g^{-1} at a current density of 400 mA g^{-1} even after 50 cycles [126]. The results indicated that dip-coating is potential to fabricate binder-free electrodes for lithium ion batteries. As could be seen from the above-mentioned, fibrous materials coated by dip-coating method is a promising research frontier for textiles energy storage. Furthermore, fibrous-based energy storage

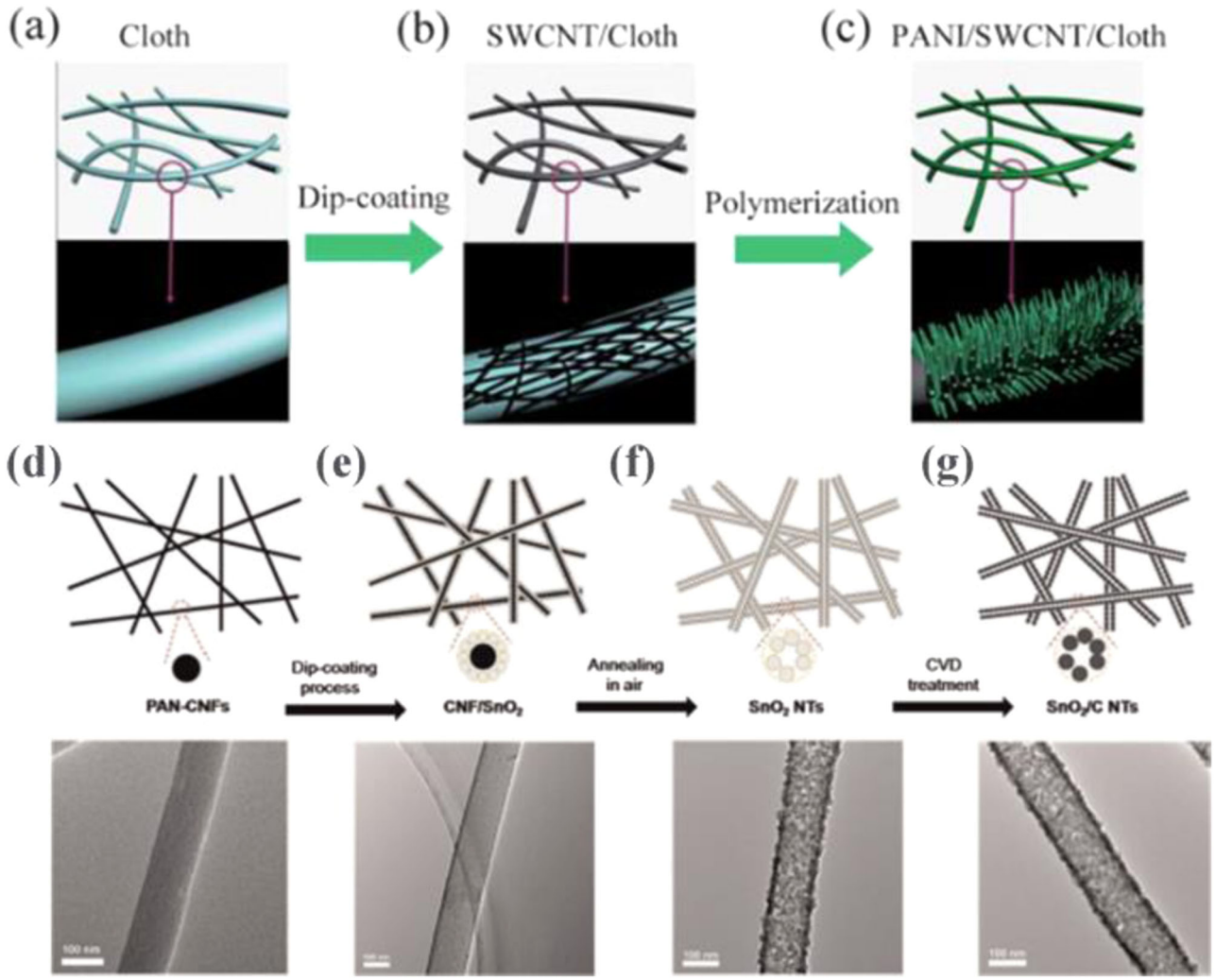

Fig. 21 **a–c** Schematic diagram of the preparation of the PANI/SWNT/cloth electrode [120]; **d–g** fabrication process of carbon fiber-based lithium ion batteries and the corresponding TEM images[126]. **a–c** Copyright 2011, Royal Society of Chemistry; **d–g** copyright 2014, Elsevier

systems with high electro-chemical activity can provide new design opportunities for wearable electronics and microelectronics devices applications.

Apart from the above-mentioned functional applications, one-dimensional photonic crystals are recently emerging multi-layered systems with spatial periodicity structure and properties. The photonic stop-band position depends on the thickness of each components, and the role of acceleration mode on the fabrication of controlled lateral gradient in photonic stop-band has been exploited, as shown in Fig. 22 [22]. The prepared photonic crystals acts as a graded reflector and cross-sectional view of the multi-layered structure are displayed in Fig. 22b, and Fig. 22a, c, respectively. It could be seen from Fig. 22d that good linear relationship is found between the minimal transmitted wavelength and dipping distance. Fig. 22e shows the transmission data of the under various dipping distance as indicated by the curves. The results indicated that the photonic stop-band could be displaced over a wide range of wavelengths without the variation of minimum transmittance values [22]. This indicated that gradient photonic crystals could be facilely fabricated by dip-coating method and potentially used as optical devices with controllable stop-band positions. The similar works concerning photonic crystals prepared by dip-coating process have also been reported [5, 127–129]. And the photonic bandgap structures were achieved mainly by the periodically alternative coating process. The applications of coated fibrous materials in the areas of bendable semiconductor fabric [69, 130], sensitive conducting composites [113], gas separation [71], flame retardant [25, 131], and water sensing [24] have also been reported. Therefore, it could be concluded that dip-coating is extremely promising in the functional applications of various fields.

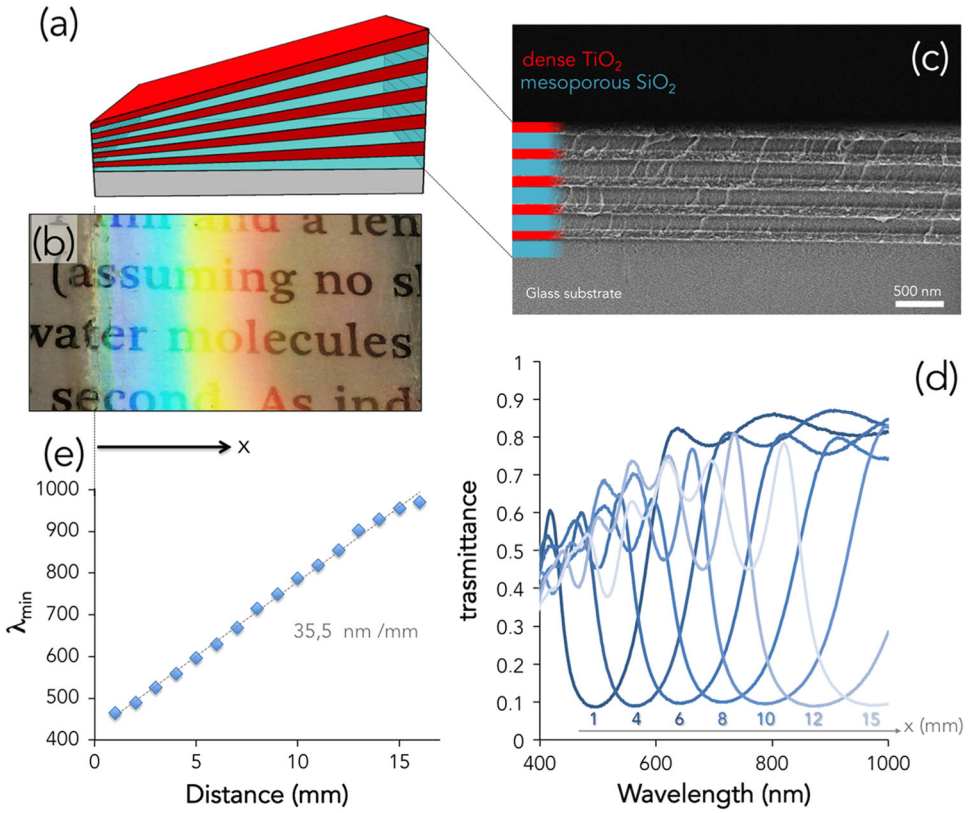

Fig. 22 **a** Illustration of the graded 1D photonic crystal; **b** optical photograph of graded 1D photonic crystal on glass substrate; **c** SEM-FEG micrograph of the five pair system; **d** UV-vis transmission spectra of the graded photonic crystal for increasing x values; **e** plot of the photonic stop-band position as a function of distance in the x-direction [22]. Copyright 2014, American Chemical Society

5 Summary

In this review, we have summarized the theoretical basis, modified dip-coating methods and various functional applications of dip-coating for fibrous materials. As it is known from theoretical analysis and established models, the deposition of coated films mainly relies on the gravity-induced viscous drag opposing the adhesion of the fluid on the substrate. The key issue of dip-coating for films deposition is the evaporation process of coating solutions, thus the above-mentioned various recently developed dip-coating methods are all based on the well control of evaporation process. Both intrinsic variables of coating solutions, including concentration, viscosity, surface tension and coating compositions, and extrinsic factors, such as temperature, withdraw speed, and external field have remarkable effects on the evaporation. Therefore, the development of advanced dip-coating techniques should concentrated on the evaporation processes, especially the chemical/physical interaction between fibrous surface and coating solutions. It can be seen from reported works that the influential factors of withdrawal speed, solution concentration, viscosity, and temperature have been mostly studied. In addition, the methods of external field assisted dip-coating have also been investigated, such as the above-mentioned vacuum-assisted and spin-assisted dip-coating for better deposited films onto substrate. Photo-assisted, template-assisted, and inverse dipping for fibrous materials that are further developed according to the well control on the wetting and evaporation process of coating solutions. Vacuum-assisted and spin-assisted dip-coating process could be attributed to the physical auxiliary effect, while photo-assisted dip-coating is the photochemical effect for solution evaporation and film deposition. However, the assist of magnetic field and electric field for dip-coating have not been reported, through the effects of magnetic/electric for solutions have been investigated. In the opinion of authors, magnetic field and electric field assisted for dipping process are promising research directions for dip-coating fibrous materials. Future works in this field have to shed light on the potential fabrication of well-controlled films with smart external field response.

The applications of dip-coating fibrous materials, including self-cleaning, oil–water separation, electrical conductivity, and energy storage devices have been reviewed. It should be noted that the dip-coating functionalization of fibrous materials was achieved mainly by changing the composition of coating solutions. The mostly studied approach is the incorporation of well-dispersed nanoparticles into polymeric-based aqueous coating solutions. Furthermore, the improvement of dip-coating methods also contribute to the functional applications of fibrous materials. Especially, the multi-layered dip-coating process could facilitate the uniform deposition of films onto fibrous

substrate, and achieve the integration of different layers. We believe that more deposited films with novel functions could be fabricated in the future, which by fully exploring the potential advantages of dip-coating.

Compliance with ethical standards

Conflict of interest The authors declare that they have no competing interests.

Reference

1. Ceratti DR, Louis B, Paquez X, Faustini M, Grosso D (2015) A new dip coating method to obtain large-surface coatings with a minimum of solution. Adv Mater 27(34): 4958–4962
2. Gaulding EA, Diroll BT, Goodwin ED, Vrtis ZJ, Kagan CR, Murray CB (2015) Deposition of wafer-scale single-component and binary nanocrystal superlattice thin films via dip-coating. Adv Mater 27(18):2846–2851
3. Dey M, Doumenc F, Guerrier B (2016) Numerical simulation of dip-coating in the evaporative regime. Eur Phys J E 39(2):19
4. Lu YF, Ganguli R, Drewien CA, Anderson MT, Brinker CJ, Gong WL, Guo YX, Soyez H, Dunn B, Huang MH, Zink JI (1997) Continuous formation of supported cubic and hexagonal mesoporous films by sol gel dip-coating. Nature 389(6649): 364–368
5. Almeida RM, Goncalves MC, Portal S (2004) Sol-gel photonic bandgap materials and structures. J Non-Cryst Solids 345: 562–569
6. Lii DF, Huang JL, Tsui LJ, Lee SM (2002) Formation of BN films on carbon fibers by dip-coating. Surf Coat Technol 150(2-3): 269–276
7. Wu YC, Parola S, Marty O, Mugnier J (2004) Elaboration, structural characterization and optical properties of the yttrium alkoxide derived Y2O3 planar optical waveguides. Opt Mater 27 (1):21–27
8. Mehner A, Datchary W, Bleil N, Zoch HW, Klopfstein MJ, Lucca DA (2005) The influence of processing on crack formation, microstructure, density and hardness of sol-gel derived zirconia films. J Sol-Gel Sci Technol 36(1):25–32
9. Hynek J, Kalousek V, Zouzelka R, Bezdicka P, Dzik P, Rathousky J, Demel J, Lang K (2014) High photocatalytic activity of transparent films composed of ZnO nanosheets. Langmuir 30(1):380–386
10. Cisneros-Zevallos L, Krochta JM (2003) Dependence of coating thickness on viscosity of coating solution applied to fruits and vegetables by dipping method. J Food Sci 68(2):503–510
11. Guglielmi M, Colombo P, Peron F, Esposti LMD (1992) Dependence of thickness on the withdrawal speed for SiO 2 and TiO 2 coatings obtained by the dipping method. J Mater Sci 27 (18):5052–5056
12. Guglielmi M, Zenezini S (1990) The thickness of sol-gel silica coatings obtained by dipping. J Non-Cryst Solids 121(1–3): 303–309
13. Jittavanich K, Clemons CB, Kreider KL, Aljarrah M, Evans E, Young GW (2010) Modeling, simulation and fabrication of coated structures using the dip coating technique. Chem Eng Sci 65(23):6169–6180
14. Roland S, Pellerin C, Bazuin CG, Prud'homme RE (2012) Evolution of small molecule content and morphology with dip-coating rate in supramolecular PS-P4VP thin films. Macromolecules 45(19):7964–7972
15. Roland S, Gamys CG, Grosrenaud J, Boisse S, Pellerin C, Prud'homme RE, Bazuin CG (2015) Solvent Influence on thickness, composition, and morphology variation with dip-coating rate in supramolecular PS-b-P4VP thin films. Macromolecules 48(14):4823–4834
16. Faustini M, Louis B, Albouy PA, Kuemmel M, Grosso D (2010) Preparation of sol-gel films by dip-coating in extreme conditions. J Phys Chem C 114(17):7637–7645
17. Faustini M, Boissiere C, Nicole L, Grosso D (2014) From chemical solutions to inorganic nanostructured materials: a journey into evaporation-driven processes. Chem Mater 26(1):709–723
18. Grosso D (2011) How to exploit the full potential of the dip-coating process to better control film formation. J Mater Chem 21(43):17033–17038
19. Lee CH, Lu YF, Shen AQ (2006) Evaporation induced self assembly and rheology change during sol-gel coating. Phys Fluids 18(5):052105
20. Uchiyama H, Shimaoka D, Kozuka H (2012) Spontaneous pattern formation based on the coffee-ring effect for organic-inorganic hybrid films prepared by dip-coating: effects of temperature during deposition. Soft Matter 8(44):11318–11322
21. Wei Q, Achazi K, Liebe H, Schulz A, Noeske PLM, Grunwald I, Haag R (2014) Mussel-Inspired dendritic polymers as universal multifunctional coatings. Angew Chem Int Edit 53(43):11650–11655
22. Faustini M, Ceratti DR, Louis B, Boudot M, Albouy PA, Boissiere C, Grosso D (2014) Engineering functionality gradients by dip coating process in acceleration mode. ACS Appl Mater Interfaces 6(19):17102–17110
23. Zhang XR, Pei XQ, Wang QH, Wang TM (2015) Friction and wear of potassium titanate whisker filled carbon fabric/phenolic polymer composites. J Tribol Trans Asme 137(1):011605
24. Qi HS, Liu JW, Deng YH, Gao SL, Mader E (2014) Cellulose fibres with carbon nanotube networks for water sensing. J Mater Chem A 2(15):5541–5547
25. Zhang QH, Zhang W, Huang JY, Lai YK, Xing TL, Chen GQ, Jin WR, Liu HZ, Sun B (2015) Flame retardance and thermal stability of wool fabric treated by boron containing silica sols. Mater Design 85:796–799
26. Foruzanmehr M, Vuillaume PY, Robert M, Elkoun S (2015) The effect of grafting a nano-TiO2 thin film on physical and mechanical properties of cellulosic natural fibers. Mater Design 85:671–678
27. Roberts M, Huang AF, Johns P, Owen J (2013) Dip-spin coating of reticulated vitreous carbon with composite materials to act as an electrode for 3D microstructured lithium ion batteries. J Power Sources 224:250–259
28. Pu DF, Zhou WX, Li Y, Chen J, Chen JY, Zhang HM, Mi BX, Wang LH, Ma YW (2015) Order-enhanced silver nanowire networks fabricated by two-step dip-coating as polymer solar cell electrodes. RSC Adv 5(122):100725–100729
29. Zhao XL, Zheng BN, Huang TQ, Gao C (2015) Graphene-based single fiber supercapacitor with a coaxial structure. Nanoscale 7 (21):9399–9404
30. Pan XL, Stroh N, Brunner H, Xiong GX, Sheng SS (2003) Deposition of sol-gel derived membranes on Al2O3 hollow fibers by a vacuum-assisted dip-coating process. J Membrane Sci 226(1–2):111–118
31. Tang XN, Tian MW, Qu LJ, Zhu SF, Guo XQ, Han GT, Sun KK, Hu XL, Wang YJ, Xu XQ (2015) Functionalization of cotton fabric with graphene oxide nanosheet and polyaniline for conductive and UV blocking properties. Synthetic Met 202:82–88
32. Kafizas A, Parry SA, Chadwick AV, Carmalt CJ, Parkin IP (2013) An EXAFS study on the photo-assisted growth of silver nanoparticles on titanium dioxide thin-films and the

identification of their photochromic states. Phys Chem Chem Phys 15(21):8254–8263
33. Niu YG, Zhang X, Pan WZ, Zhao JP, Li Y (2014) Enhancement and wettability of self-assembled GO sheets as interfacial layers of CF/PI composites. RSC Adv 4(15):7511–7515
34. Blaese D, Garcia DE, Guglielmi P, Hotza D, Fredel MC, Janssen R (2015) ZrO_2 fiber-matrix interfaces in alumina fiber-reinforced model composites. J Eur Ceram Soc 35(5): 1593–1598
35. Church JS, Voda AS, Sutti A, George J, Fox BL, Magniez K (2015) A simple and effective method to ameliorate the interfacial properties of cellulosic fibre based bio-composites using poly (ethylene glycol) based amphiphiles. Eur Poly J 64:70–78
36. Agnihotri P, Basu S, Kar KK (2011) Effect of carbon nanotube length and density on the properties of carbon nanotube-coated carbon fiber/polyester composites. Carbon 49(9):3098–3106
37. Li XG, Shen J (2011) A facile two-step dipping process based on two silica systems for a superhydrophobic surface. Chem Comm 47(38):10761–10763
38. Wang H, Zakirov A, Yuldashev SU, Lee J, Fu D, Kang T (2011) ZnO films grown on cotton fibers surface at low temperature by a simple two-step process. Mater Lett 65(9):1316–1318
39. Liu YT, Long T, Tang S, Sun JL, Zhu ZA, Guo YP (2014) Biomimetic fabrication and biocompatibility of hydroxyapatite/chitosan nanohybrid coatings on porous carbon fiber felts. Mater Lett 128:31–34
40. Janjic S, Kostic M, Vucinic V, Dimitrijevic S, Popovic K, Ristic M, Skundric P (2009) Biologically active fibers based on chitosan-coated lyocell fibers. Carbohyd Polym 78(2):240–246
41. Navarro CH, Moreno KJ, Chávez-Valdez A, Louvier-Hernández F, García-Miranda JS, Lesso R, Arizmendi-Morquecho A (2012) Friction and wear properties of poly(methyl methacrylate)–hydroxyapatite hybrid coating on UHMWPE substrates. Wear 282-283:76–80
42. Morales-Nieto V, Navarro CH, Moreno KJ, Arizmendi-Morquecho A, Chávez-Valdez A, García-Miranda S, Louvier-Hernández JF (2013) Poly(methyl methacrylate)/carbonated hydroxyapatite composite applied as coating on ultra high molecular weight polyethylene. Prog Org Coat 76(1):204–208
43. Subba-Rao V, Sudakar C, Esmacher J, Pantea M, Naik R, Hoffmann PM (2009) Improving a high-resolution fiber-optic interferometer through deposition of a TiO2 reflective coating by simple dip-coating. Rev Sci Instrum 80(11):115104
44. Wang XL, Pan DC, Weng D, Low CY, Rice L, Han JY, Lu YF (2010) A general synthesis of Cu-In-S based multicomponent solid-solution nanocrystals with tunable band gap, size, and structure. J Phys Chem C 114(41):17293–17297
45. Gu X, Trusty PA, Butler EG, Ponton CB (2000) Deposition of zirconia sols on woven fibre preforms using a dip-coating technique. J Eur Ceram Soc 20(6):675–684
46. Desimone D, Dlouhy I, Lee WE, Koch D, Horvath J, Boccaccini AR (2010) Optically-transparent oxide fibre-reinforced glass matrix composites. J Non-Cryst Solids 356(44–49):2591–2597
47. Nguyen HT, Miao L, Tanemura S, Tanemura M, Toh S, Kaneko K, Kawasaki M (2004) Structural and morphological characterization of anatase TiO_2 coating on α-Alumina scale fiber fabricated by sol-gel dip-coating method. J Cryst Growth 271(1–2):245–251
48. Yin YJ, Wang CX (2011) Multifunctional performances of nanocomposite SiO_2/TiO_2 doped cationic EBODAC film coated on natural cellulose matrix. J Sol-Gel Sci Technol 59(1):36–42
49. Yin YJ, Wang CX (2013) Water-repellent functional coatings through hybrid SiO_2/HTEOS/CPTS sol on the surfaces of cellulose fibers. Colloids Surf A 417:120–125
50. Yin YJ, Li T, Fan F, Zhao CY, Wang CX (2013) Dynamically modifiable wettability comparisons of the hydrophilic and hydrophobic substrates coated with F/TiO_2 hybrid sol by UV irradiation. Appl Surf Sci 283:482–489
51. Yin YJ, Wang CX, Shen QK, Zhang GF, Galib CMA (2013) Surface deposition on cellulose substrate via cationic SiO_2/TiO_2 hybrid sol for transfer printing using disperse dye. Ind Eng Chem Res 52(31):10656–10663
52. Rehana P, Ummer RB, Thevenot Camille, Rouxel Didier, Thomas Sabu, Kalarikkal N (2016) Electric, magnetic, piezoelectric and magnetoelectric studies of phase pure ($BiFeO_3$–$NaNbO_3$)–(P(VDF-TrFE)) nanocomposite films prepared by spin coating. RSC Adv 6:28069
53. Chen RJ, Huang M, Huang WZ, Shen Y, Lin YH, Nan CW (2014) Sol-gel derived Li-La-Zr-O thin films as solid electrolytes for lithium-ion batteries. J Mater Chem A 2 (33):13277–13282
54. Jo JW, Jung JW, Lee JU, Jo WH (2010) Fabrication of highly conductive and transparent thin films from single-walled carbon nanotubes using a new non-ionic surfactant via spin coating. ACS Nano 4(9):5382–5388
55. Wang XD, Shi F, Gao XX, Fan CM, Huang W, Feng XS (2013) A sol-gel dip/spin coating method to prepare titanium oxide films. Thin Solid Films 548:34–39
56. Emslie AG, Bonner FT, Peck LG (1958) Flow of a viscous liquid on a rotating disk. J Appl Phys 29(5):858
57. Harwood DW, Taylor ER, Moore R, Payne D (2003) Fabrication of fluoride glass planar waveguides by hot dip spin coating. J Non-Cryst Solids 332(1–3):190–198
58. Cho J, Char K, Hong JD, Lee KB (2001) Fabrication of highly ordered multilayer films using a spin self-assembly method. Adv Mater 13(14):1076–1078
59. Li Y, Wang X, Sun JQ (2012) Layer-by-layer assembly for rapid fabrication of thick polymeric films. Chem Soc Rev 41 (18):5998–6009
60. Chiarelli PA, Johal MS, Casson JL, Roberts JB, Robinson JM, Wang HL (2001) Controlled fabrication of polyelectrolyte multilayer thin films using spin-assembly. Adv Mater 13 (15):1167–1171
61. Kharlampieva E, Kozlovskaya V, Chan J, Ankner JF, Tsukruk VV (2009) Spin-assisted layer-by-layer assembly: variation of stratification as studied with neutron reflectivity. Langmuir 25 (24):14017–14024
62. Wang YH, Liu J, Wu X, Yang B (2014) Adhesion enhancement of indium tin oxide (ITO) coated quartz optical fibers. Appl Surf Sci 308:341–346
63. Nie WY, Li Y, Zhou W, Liu JW, Carroll DL (2012) Multi-layer deposition of conformal, transparent, conducting oxide films for device applications. Thin Solid Films 520(11):4008–4015
64. Dolay A, Courtois C, d'Astorg S, Rguiti M, Petitniot JL, Leriche A (2014) Fabrication and characterization of metal core piezoelectric fibres by dip coating process. J Eur Ceram Soc 34 (12):2951–2957
65. Nagao D, Kameyama R, Matsumoto H, Kobayashi Y, Konno M (2008) Single- and multi-layered patterns of polystyrene and silica particles assembled with a simple dip-coating. Colloids Surf A 317(1–3):722–729
66. Barletta M, Trovalusci F, Gisario A, Venettacci S (2013) New ways to the manufacturing of pigmented multi-layer protective coatings. Surf Coat Technol 232:860–867
67. Zhou H, Wang H, Niu H, Gestos A, Lin T (2013) Robust, self-healing superamphiphobic fabrics prepared by two-step coating of fluoro-containing polymer, fluoroalkyl silane, and modified silica nanoparticles. Adv Funct Mater 23(13):1664–1670
68. Tanaka DAP, Tanco MAL, Nagase T, Okazaki J, Wakui Y, Mizukami F, Suzuki TM (2006) Fabrication of hydrogen-permeable composite membranes packed with palladium nanoparticles. Adv Mater 18(5):630–632

69. Smith DA, Holmberg VC, Korgel BA (2010) Flexible germanium nanowires: ideal strength, room temperature plasticity, and bendable semiconductor fabric. ACS Nano 4(4):2356–2362
70. Zhang XZ, Lin B, Ling YH, Dong YC, Meng GY, Liu XQ (2010) An anode-supported hollow fiber solid oxide fuel cell with (Pr0.5Nd0.5)(0.7)Sr0.3MnO_3-delta-YSZ composite cathode. J Alloys Compd 497(1–2):386–389
71. Bazzarelli F, Bernardo P, Tasselli F, Clarizia G, Dzyubenko VG, Vdovin P, Jansen JC (2011) Multilayer composite SBS membranes for pervaporation and gas separation. Sep Purif Technol 80(3):635–642
72. Samad YA, Li YQ, Alhassan SM, Liao K (2015) Novel graphene foam composite with adjustable sensitivity for sensor applications. ACS Appl Mater Interfaces 7(17):9195–9202
73. Ramasubramanian K, Severance MA, Dutta PK, Ho WSW (2015) Fabrication of zeolite/polymer multilayer composite membranes for carbon dioxide capture: Deposition of zeolite particles on polymer supports. J Colloid Interf Sci 452:203–214
74. Koga H, Nogi M, Komoda N, Nge TT, Sugahara T, Suganuma K (2014) Uniformly connected conductive networks on cellulose nanofiber paper for transparent paper electronics. NPG Asia Mater 6:e93
75. Matsuzaki Y, Hishinuma M, Yasuda I (1999) Photo-excitation effects on pyrolysis of metallo-organic precursors for yttria-stabilized zirconia thin films. Thin Solid Films 354(1–2):38–42
76. Kafizas A, Dunnill CW, Parkin IP (2011) The relationship between photocatalytic activity and photochromic state of nanoparticulate silver surface loaded titanium dioxide thin-films. Phys Chem Chem Phys 13(30):13827–13838
77. Brasse G, Restoin C, Soul D, Blondy JM (2011) Rheology study of silica-zirconia sols for elaboration of silica-zirconia nanostructured optical fibers by inverse dip coating. J Phys Chem C 115(1):248–252
78. Dewalque J, Cloots R, Mathis F, Dubreuil O, Krins N, Henrist C (2011) TiO_2 multilayer thick films (up to 4 mu m) with ordered mesoporosity: influence of template on the film mesostructure and use as high efficiency photoelectrode in DSSCs. J Mater Chem 21(20):7356–7363
79. Takahashi T, Matsutani A, Shoji D, Nishioka K, Sato M, Isobe T, Nakajima A, Matsushita S (2015) Microfabrication for a polystyrene quadrupole by template-assisted self-assembly. Colloids Surf A 484:75–80
80. Spotnitz ME, Ryan D, Stone HA (2004) Dip coating for the alignment of carbon nanotubes on curved surfaces. J Mater Chem 14(8):1299–1302
81. Huang J, Fan R, Connor S, Yang P (2007) One-step patterning of aligned nanowire arrays by programmed dip coating. Angew Chem Int Edit 46(14):2414–2417
82. Kang TJ, Yoon JW, Kim DI, Kum SS, Huh YH, Hahn JH, Moon SH, Lee HY, Kim YH (2007) Sandwich-type laminated nanocomposites developed by selective dip-coating of carbon nanotubes. Adv Mater 19(3):427–432
83. Ding DH, Zhou WC, Luo F, Chen ML, Zhu DM (2012) Dip-coating of boron nitride interphase and its effects on mechanical properties of SiCf/SiC composites. Mater Sci Eng A 543:1–5
84. Qi KH, Daoud WA, Xin JH, Mak CL, Tang WZ, Cheung WP (2006) Self-cleaning cotton. J Mater Chem 16(47):4567–4574
85. Velasco E, Baldovino-Medrano VG, Gaigneaux EM, Giraldo SA (2016) Development of an efficient strategy for coating TiO_2 on polyester-cotton fabrics for bactericidal applications. Topics Catal 59(2–4):378–386
86. Doganli G, Yuzer B, Aydin I, Gultekin T, Con AH, Selcuk H, Palamutcu S (2016) Functionalization of cotton fabric with nanosized TiO_2 coating for self-cleaning and antibacterial property enhancement. J Coat Technol Res 13(2):257–265
87. Moafi HF, Shojaie AF, Zanjanchi MA (2011) Titania and titania nanocomposites on cellulosic fibers: Synthesis, characterization and comparative study of photocatalytic activity. Chem Eng J 166(1):413–419
88. Moafi HF, Shojaie AF, Zanjanchi MA (2013) Photoactive behavior of polyacrylonitrile fibers based on silver and zirconium co-doped titania nanocomposites: synthesis, characterization, and comparative study of solid-phase photocatalytic self-cleaning. J Appl Polym Sci 127(5):3778–3789
89. Yuranova T, Mosteo R, Bandara J, Laub D, Kiwi J (2006) Self-cleaning cotton textiles surfaces modified by photoactive SiO_2/TiO_2 coating. J Molecular Catal A 244(1–2):160–167. doi:10.1016/j.molcata.2005.08.059
90. Qi KH, Chen XQ, Liu YY, Xin JH, Mak CL, Daoud WA (2007) Facile preparation of anatase/SiO_2 spherical nanocomposites and their application in self-cleaning textiles. J Mater Chem 17 (33):3504–3508
91. Wang RH, Wang XW, Xin JH (2010) Advanced visible-light-driven self-cleaning cotton by Au/TiO_2/SiO_2 photocatalysts. ACS Appl Mater Interfaces 2(1):82–85
92. Nateghi MR, Shateri-Khalilabad M (2015) Silver nanowire-functionalized cotton fabric. Carbohyd Polym 117:160–168
93. Zeng C, Wang HX, Zhou H, Lin T (2015) Self-cleaning, superhydrophobic cotton fabrics with excellent washing durability, solvent resistance and chemical stability prepared from an SU-8 derived surface coating. RSC Adv 5(75): 61044–61050
94. Liu YY, Wang XW, Qi KH, Xin JH (2008) Functionalization of cotton with carbon nanotubes. J Mater Chem 18(29):3454–3460
95. Yin YJ, Guo N, Wang CX, Rao QQ (2014) Alterable superhydrophobic-superhydrophilic wettability of fabric substrates decorated with ion-TiO_2 coating via ultraviolet radiation. Ind Eng Chem Res 53(37):14322–14328
96. Xue Z, Cao Y, Liu N, Feng L, Jiang L (2014) Special wettable materials for oil/water separation. J Mater Chem A 2(8): 2445–2460
97. Yoon H, Na SH, Choi JY, Latthe SS, Swihart MT, Al-Deyab SS, Yoon SS (2014) Gravity-driven hybrid membrane for oleophobic-superhydrophilic oil water separation and water purification by graphene. Langmuir 30(39):11761–11769
98. Karimnezhad H, Rajabi L, Salehi E, Derakhshan AA, Azimi S (2014) Novel nanocomposite Kevlar fabric membranes: fabrication characterization, and performance in oil/water separation. Appl Surf Sci 293:275–286
99. Wu L, Zhang JP, Li BC, Wang AQ (2014) Mechanical- and oil-durable superhydrophobic polyester materials for selective oil absorption and oil/water separation. J Colloid Interface Sci 413:112–117
100. Li KQ, Zeng XR, Li HQ, Lai XJ, Xie H (2014) Facile fabrication of superhydrophobic filtration fabric with honeycomb structures for the separation of water and oil. Mater Lett 120:255–258
101. Zhu XT, Zhang ZZ, Ge B, Men XH, Zhou XY, Xue QJ (2014) A versatile approach to produce superhydrophobic materials used for oil-water separation. J Colloid Interface Sci 432:105–108
102. Cao YZ, Liu N, Zhang WF, Feng L, Wei Y (2016) One-step coating toward multifunctional applications: oil/water mixtures and emulsions separation and contaminants. Adsorption. ACS Appl Mater Interfaces 8(5):3333–3339
103. Zhang WF, Lu X, Xin Z, Zhou CL (2015) A self-cleaning polybenzoxazine/TiO_2 surface with superhydrophobicity and superoleophilicity for oil/water separation. Nanoscale 7 (46):19476–19483
104. Kong Y, Liu Y, Xin JH (2011) Fabrics with self-adaptive wettability controlled by "light-and-dark". J Mater Chem 21 (44):17978–17987

105. Yan L, Li J, Li WJ, Zha F, Feng H, Hu DC (2016) A photo-induced ZnO coated mesh for on-demand oil/water separation based on switchable wettability. Mater Lett 163:247–249
106. Xu Z, Zhao Y, Wang H, Wang X, Lin T (2015) A super-amphiphobic coating with an ammonia-triggered transition to superhydrophilic and superoleophobic for oil-water separation. Angew Chem Int Edit 54(15):4527–4530
107. Atwa Y, Maheshwari N, Goldthorpe IA (2015) Silver nanowire coated threads for electrically conductive textiles. J Mater Chem C 3(16):3908–3912
108. Gan L, Shang S, Yuen CWM, Jiang S-x (2015) Graphene nanoribbon coated flexible and conductive cotton fabric. Compos Sci Technol 117:208–214
109. Narayanan SC, Karpagam KR, Bhattacharyya A (2015) Nano-composite coatings on cotton and silk fibers for enhanced electrical conductivity. Fibers Polym 16(6):1269–1275
110. Tang YJ, Mosseler JA, He ZB, Ni YH (2014) Imparting cellulosic paper of high conductivity by surface coating of dispersed graphite. Ind Eng Chem Res 53(24):10119–10124
111. Qin WZ, Vautard F, Drzal LT, Yu JR (2015) Mechanical and electrical properties of carbon fiber composites with incorporation of graphene nanoplateletsat the fiber-matrix interphase. Compos Part B-Eng 69:335–341
112. Wang Y, Rouabhia M, Zhang Z (2013) PPy-coated PET fabrics and electric pulse-stimulated fibroblasts. J Mater Chem B 1 (31):3789–3796
113. Hodlur RM, Rabinal MK (2014) Self assembled graphene layers on polyurethane foam as a highly pressure sensitive conducting composite. Compos Sci Technol 90:160–165
114. Jiang SJ, Zhang HB, Song SQ, Ma YW, Li JH, Lee GH, Han QW, Liu J (2015) Highly stretchable conductive fibers from few-walled carbon nanotubes coated on poly(m-phenylene isophthalamide) polymer core/shell structures. ACS Nano 9 (10):10252–10257
115. Hasan MMB, Cherif C, Foisal ABM, Onggar T, Hund RD, Nocke A (2013) Development of conductive coated polyether ether ketone (PEEK) filament for structural health monitoring of composites. Compos Sci Technol 88:76–83
116. Jost K, Dion G, Gogotsi Y (2014) Textile energy storage in perspective. J Mater Chem A 2(28):10776–10787
117. Hu L, Pasta M, Mantia FL, Cui L, Jeong S, Deshazer HD, Choi JW, Han SM, Cui Y (2010) Stretchable, porous, and conductive energy textiles. Nano lett 10(2):708–714
118. Yu G, Hu L, Vosgueritchian M, Wang H, Xie X, McDonough JR, Cui X, Cui Y, Bao Z (2011) Solution-processed graphene/MnO_2 nanostructured textiles for high-performance electrochemical capacitors. Nano lett 11(7):2905–2911
119. Xu J, Wu H, Xu C, Huang HT, Lu LF, Ding GQ, Wang HL, Liu DF, Shen GZ, Li DD, Chen XY (2013) Structural engineering for high energy and voltage output supercapacitors. Chem A Eur J 19(20):6451–6458
120. Wang K, Zhao P, Zhou XM, Wu HP, Wei ZX (2011) Flexible supercapacitors based on cloth-supported electrodes of conducting polymer nanowire array/SWCNT composites. J Mater Chem 21(41):16373–16378
121. Gui Z, Zhu HL, Gillette E, Han XG, Rubloff GW, Hu LB, Lee SB (2013) Natural cellulose fiber as substrate for supercapacitor. ACS Nano 7(7):6037–6046
122. Zhai S, Karahan HE, Wei L, Qian Q, Harris AT, Minett AI, Ramakrishna S, Ng AK, Chen Y (2016) Textile energy storage: structural design concepts, material selection and future perspectives. Energy Storage Mater 3:123–139
123. Hu LB, La Mantia F, Wu H, Xie X, McDonough J, Pasta M, Cui Y (2011) Lithium-ion textile batteries with large areal mass loading. Adv Energy Mater 1(6):1012–1017
124. Liu B, Zhang J, Wang X, Chen G, Chen D, Zhou C, Shen G (2012) Hierarchical three-dimensional ZnCo(2)O(4) nanowire arrays/carbon cloth anodes for a novel class of high-performance flexible lithium-ion batteries. Nano Lett 12(6):3005–3011
125. Lee YH, Kim JS, Noh J, Lee I, Kim HJ, Choi S, Seo J, Jeon S, Kim TS, Lee JY, Choi JW (2013) Wearable textile battery rechargeable by solar energy. Nano Lett 13(11): 5753–5761
126. Li SY, Wang Q, Xie WH, Xue S, Hou XY, He DY (2015) DIP-coating process to fabricate SnO_2/C nanotube networks as binder-free anodes for lithium ion batteries. Mater Lett 158:244–247
127. Wei NN, Han T, Deng GZ, Li JL, Du JY (2011) Synthesis and characterizations of three-dimensional ordered gold- nanoparticle-doped titanium dioxide photonic crystals. Thin Solid Films 519(8):2409–241
128. Fortes LM, Clara Goncalves M, Almeida RM (2011) Flexible photonic crystals for strain sensing. Optical Mater 33 (3):408–412
129. Fortes LM, Goncalves MC, Almeida RM (2009) Processing optimization and optical properties of 3-D photonic crystals. J Non-Cryst Solids 355(18-21):1189–1192
130. Zhukovskyi M, Sanchez-Botero L, McDonald MP, Hinestroza J, Kuno M (2014) Nanowire-functionalized cotton textiles. ACS Appl Mater Interfaces 6(4):2262–2269
131. Leistner M, Abu-Odeh AA, Rohmer SC, Grunlan JC (2015) Water-based chitosan/melamine polyphosphate multilayer nanocoating that extinguishes fire on polyester-cotton fabric. Carbohyd Polym 130:227–232